

# On the Deque and Rique Numbers of Complete and Complete Bipartite Graphs

Michael A. Bekos<sup>1</sup>, Michael Kaufmann<sup>2</sup>, Maria Eleni Pavlidi<sup>3</sup>, Xenia Rieger<sup>4</sup>,

<sup>1</sup>Department of Mathematics, University of Ioannina, Ioannina, Greece

`bekos@uoi.gr`

<sup>2</sup>Institute for Computer Science, University of Tübingen, Tübingen, Germany

`michael.kaufmann@uni-tuebingen.de`

<sup>3</sup>Department of Mathematics, University of Ioannina, Ioannina, Greece

`marialenaregie3@gmail.com`

<sup>4</sup>Institute for Computer Science, University of Tübingen, Tübingen, Germany

`xenia.rieger@student.uni-tuebingen.de`

## Abstract

Several types of linear layouts of graphs are obtained by leveraging known data structures; the most notable representatives are the stack and the queue layouts. In this content, given a data structure, one seeks to specify an order of the vertices of the graph and a partition of its edges into *pages*, such that the endpoints of the edges assigned to each page can be processed by the given data structure in the underlying order.

In this paper, we study deque and rique layouts of graphs obtained by leveraging the double-ended queue and the restricted-input double-ended queue (or deque and rique, for short), respectively. Hence, they generalize both the stack and the queue layouts. We focus on complete and complete bipartite graphs and present bounds on their deque- and rique-numbers, that is, on the minimum number of pages needed by any of these two types of linear layouts.

## 1 Introduction

Stack and queue layouts form two of the most studied types of linear layouts of graphs; they date back to 70's [8, 16] and over the years several remarkable results have been proposed in the literature [10, 15, 17, 18, 22]. For an introduction, refer to Section 2. Both layouts are defined by an underlying vertex order and an edge-partition into a certain number of so-called *pages* (*stacks* or *queues*, respectively), such that when restricting to a single page the endpoints of the edges assigned to it can be processed by the corresponding data structure in the order that appears in the underlying vertex order.

Since given a graph the natural goal is to find a layout of it that minimizes the number of used pages under the restrictions mentioned above, stack and queue layouts have naturally been leveraged to estimate the power of the respective data structures as a mean for representing graphs (for a wealth of other applications, e.g., to VLSI design and Graph Drawing, refer to [11]). The well-known *stack-number* (a.k.a. *book-thickness* or *page-number* in the literature)

of a graph corresponds to the minimum number of stacks required by any of the stack layouts of it; the queue-number of a graph is defined symmetrically. In this context, it was recently shown that the stack-number of a graph cannot always be bounded by its corresponding queue-number [9], resolving a long-standing open question by Heath, Leighton and Rosenberg [15]; the other direction is still unknown.

A data structure that generalizes both the stack and the queue is the so-called *double-ended queue* or *deque*, for short.<sup>1</sup> As a matter of fact, the most common implementations of stacks and queues are derived by restricting corresponding implementations of deques. So, in this aspect, one naturally expects that the corresponding linear layouts that are obtained by employing the deque data structure for stipulating their edge-partitions will require fewer pages (called *deques* in this content) than those of stack or queue layouts, since, obviously, the latter form a special case of the former.

However, in contrast to the literature for stack and queue layouts, the corresponding literature for deque layouts is significantly reduced. To the best of our knowledge, there exists only one work introducing and studying deque layouts by Auer et al. [3], who provide a complete characterization of the graphs admitting 1-deque layouts (that is, deque layouts with a single deque): a graph admits a 1-deque layout if and only if it is a spanning subgraph of a planar graph with a Hamiltonian path; see also [2]. Even though the *deque-number* of a graph (that is, the minimum number of deques required by any of the deque layouts of the graph) has not been explicitly studied so far in the literature as a graph parameter, from the characterization by Auer et al. one can easily deduce the following.

**Observation 1** (Auer et al. [3]). *The deque-number of a graph is at most half of its stack-number.*

Note that the queue-number is also a trivial upper bound on the deque-number of a graph. Observation 1, however, immediately implies improved upper bounds on the deque-number of several graph classes, e.g., the deque-number of the complete graph  $K_n$  is at most  $\lceil \frac{n}{4} \rceil$  [8], the deque-number of the complete graph  $K_{n,n}$  is at most  $\lceil \frac{\lfloor 2n/3 \rfloor + 1}{2} \rceil$  [12], while the deque-number of treewidth- $k$  graphs is at most  $\lceil \frac{k+1}{2} \rceil$  [14]. Also, since there exist maximal planar graphs that do not have a Hamiltonian path (e.g., the  $n$ -vertex ones with an independent set of size greater than  $\frac{n}{2} + 2$ ), it follows by a well-known result by Yannakakis [22] that the deque-number of planar graphs is 2; see also [6, 23].

Another consequence of Observation 1 is that deque layouts cannot be characterized by means of forbidden patterns in the underlying linear order, as it is the case, e.g., for stack and queue layouts [16, 20]; the former do not allow two edges of the same page to cross (i.e., to have alternating endpoints), while in the latter no two edges of the same page nest (i.e., have nested endpoints). The reason for the lack of such a characterization for deque layouts is the fact that maximal planar graphs with a Hamiltonian path are the maximal graphs that admit 2-stack layouts and these layouts do not admit characterizations in terms of forbidden patterns in the underlying linear order [21]. A characterization in terms of forbidden patterns is possible, however, for a special type of deque layouts, which were recently introduced and are referred to as *rique layouts* [4], since the underlying data structure is of restricted input (so-called *restricted-input double-ended queue* or *rique*,<sup>2</sup> for short): a graph admits a 1-rique layout if and only if it admits a vertex order  $\prec$  avoiding three edges  $(a, a')$ ,  $(b, b')$  and  $(c, c')$  such that  $a \prec b \prec c \prec b' \prec \{a', c'\}$ .

<sup>1</sup>While in a stack insertions and removals only occur at its head and in a queue insertions only occur at its head and removals only at its tail, a deque supports insertions and removals both at its head and its tail.

<sup>2</sup>Formally, in a rique insertions occur only at the head, and removals occur both at the head and the tail. Thus, it is a special case of a deque and a generalization of a stack or of a queue.

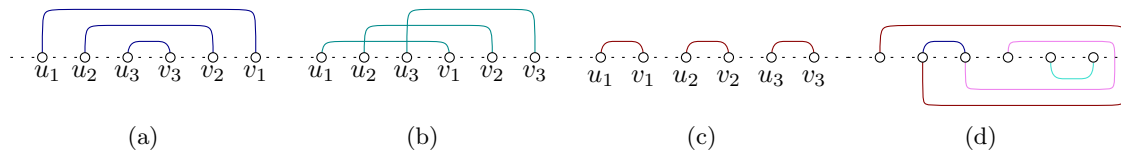


Figure 1: Illustration of: (a) a 3-rainbow, (b) a 3-twist, (c) a 3-necklace, and (d) a deque.

**Our contribution.** In this work, we present bounds on the deque- and rique-numbers of complete and complete bipartite graphs. Especially, for deque layouts, the main research question that triggered our work is whether it is possible to obtain better bounds than the obvious ones that one can deduce from Observation 1 (or in other words, whether the deque data structure is more powerful for representing graphs than two stacks). Surprisingly enough, we prove that for the case of complete graphs, this is not the case (see Theorem 3), while for the case of complete bipartite graphs our upper bound shows that an improvement by a constant number is possible (to achieve this, however, we describe a rather complicated edge-to-deques assignment; see Theorem 6). For rique layouts, our contribution is twofold. First, we improve the upper bound on the rique-number of  $K_n$  from  $\lceil \frac{n}{3} \rceil$  [4] to  $\lfloor \frac{n-1}{3} \rfloor$  (see Theorem 5), which we prove to be tight up to  $n = 30$  using an SAT-based approach (see Section 5). We complete our study with an upper bound of  $\lfloor \frac{n-1}{2} \rfloor - 1$  on the rique-number of  $K_{n,n}$ .

## 2 Preliminaries

A *vertex order*  $\prec$  of a graph  $G$  is a total order of its vertices, such that for any two vertices  $u$  and  $v$  of  $G$ ,  $u \prec v$  if and only if  $u$  precedes  $v$  in the order. We write  $[u_1, \dots, u_k]$  if and only if  $u_i \prec u_{i+1}$  for all  $1 \leq i \leq k-1$ . Let  $F$  be a set of  $k \geq 2$  pairwise independent edges  $(u_i, v_i)$  of  $G$ , that is,  $F = \{(u_i, v_i); i = 1, \dots, k\}$ . If the order is  $[u_1, \dots, u_k, v_k, \dots, v_1]$ , then we say that the edges of  $F$  form a *k-rainbow*, while if the order is  $[u_1, v_1, \dots, u_k, v_k]$ , then the edges of  $F$  form a *k-necklace*. The edges of  $F$  form a *k-twist*, if the order is  $[u_1, \dots, u_k, v_1, \dots, v_k]$ ; see Fig. 1. Two independent edges that form a 2-twist (2-rainbow, 2-necklace) are commonly referred to as *crossing* (*nested*, *disjoint*, respectively).

A *stack* is a set of pairwise non-crossing edges in  $\prec$ , while a *queue* is a set of pairwise non-nested edges in  $\prec$ . A *rique* is a set of edges in which no three edges  $(a, a')$ ,  $(b, b')$  and  $(c, c')$  with  $a \prec b \prec c \prec b' \prec \{a', c'\}$  exists in  $\prec$ . A deque is more difficult to describe due to the absence of a forbidden pattern. A relatively-simple way is the following. Assume that the vertices of a graph are arranged on a horizontal line  $\ell$  from left to right according to  $\prec$  (say, w.l.o.g., equidistantly). Then, each edge  $(v_i, v_j)$  with  $v_i \prec v_j$  can be represented either (i) as a semi-circle that is completely above or completely below  $\ell$  connecting  $u_i$  and  $u_j$ , or (ii) as two semi-circles on opposite sides of  $\ell$ , one that starts at  $u_i$  and ends at a point  $p_{ij}$  of  $\ell$  to the right of the last vertex of  $\prec$  and one that starts at point  $p_{ij}$  and ends at  $u_j$ . With these in mind, a deque is a set of edges each of which can be represented with one of the two types (i) or (ii) that avoids crossings (such a representation is called *cylindric* in [3]); see Fig. 1d. A deque further allows classifying the edges into four categories: head-head, tail-tail, head-tail and tail-head; refer to the blue, light-blue, red and light-red edges of Fig. 1d, respectively. A *head-head* (*tail-tail*) edge is a type-(i) edge drawn above (below, respectively)  $\ell$ . Symmetrically, a *head-tail* (*tail-head*) edge is a type-(ii) edge whose first part is above (below)  $\ell$ , while its second part is below (above, respectively)  $\ell$ . Given a deque layout  $L$  and a set of edges  $E$ , we write  $E_x$  to denote that all edges of  $E$  are of type- $x$  in  $L$ , where  $x \in \{hh, tt, ht, th\}$ .

In view of the above definitions, a rique can be equivalently defined as a deque without tail-tail and tail-head edges [4]. Also, it is not difficult to see that the subset of the head-head or tail-tail edges of a deque induce a stack in  $\prec$ , while the set of the head-tail or tail-head edges of a deque induces a queue in  $\prec$ .

Since we focus on complete and complete bipartite graphs, for representing their linear layouts we use a convenient way first introduced in [19] and subsequently used in several works [12, 13, 1]. Let  $\prec$  be an order of the  $n$  vertices  $v_1, \dots, v_n$  of a graph  $G$  such that  $v_1 \prec \dots \prec v_n$ . Then, each edge  $(v_i, v_j)$  of  $G$  with  $i < j$  is mapped to point  $(i, j)$  of the  $n \times n$  grid  $H = [1, n] \times [1, n]$ . A set of head-head or tail-tail edges of the same page (deque or rique) corresponds to a set of points on  $H$  whose union forms a monotonically decreasing curve on  $H$  [19]. A set of head-tail or tail-head edges of the same page (deque or rique) corresponds to a set of points on  $H$  whose union forms a monotonically increasing path on  $H$  [1]. If a deque contains head-tail and tail-head edges, special care is needed to avoid configurations not appearing in a cylindric layout.

### 3 Complete graphs

In this section, we study the deque- and rique-numbers of the complete graph  $K_n$ . As already mentioned, Observation 1 implies that  $\lceil \frac{n}{4} \rceil$  is an easy-to-obtain upper bound on the deque-number of  $K_n$ . In the following, we prove that this bound is tight. To do so, we first give an estimation on the maximum number of edges that a graph admitting a  $k$ -deque layout can have.

**Lemma 2.** *A graph with  $n$  vertices admitting a deque layout with  $k$  pages has at most  $(2k + 1)n - 5k - 1$  edges.*

*Proof.* Let  $G$  be a graph with  $n$  vertices admitting a  $k$ -deque layout. Let also  $v_1 \prec \dots \prec v_n$  be the linear order of the vertices of  $G$ . Since each deque induces a planar graph, it has at most  $3n - 6$  edges. However, the  $n - 1$  so-called *spine edges*  $(v_i, v_{i+1})$ ,  $i = 1, \dots, n - 1$  can be added as head-head edges to every deque of the layout. So, every deque has at most  $2n - 5$  non-spine edges. Hence, in total  $G$  has  $(2n - 5)k + n - 1$  edges.  $\square$

We are now ready to prove that the deque-number of the complete graph  $K_n$  is  $\lceil \frac{n}{4} \rceil$ .

**Theorem 3.** *The deque-number of  $K_n$  is  $\lceil \frac{n}{4} \rceil$ .*

*Proof.* The upper bound follows from Observation 1 and [8]. For the lower bound, let  $k$  be the number of deques of  $K_n$ . Since  $K_n$  has  $\frac{n(n-1)}{2}$  edges, by Lemma 2, it follows that  $(2k + 1)n - 5k - 1 \geq \frac{n^2 - n}{2}$ , which implies:

$$k \geq \frac{n^2 - 3n + 2}{4n - 10} \quad \text{for } n \geq 3$$

To complete the proof of the theorem, we next show that  $\lceil \frac{n^2 - 3n + 2}{4n - 10} \rceil = \lceil \frac{n}{4} \rceil$ . We do this in two steps. We first prove that  $\lceil \frac{n^2 - 3n + 2}{4n - 10} \rceil - \lceil \frac{n}{4} \rceil \leq 0$ .

$$\left\lceil \frac{n^2 - 3n + 2}{4n - 10} \right\rceil - \left\lceil \frac{n}{4} \right\rceil \leq \left\lceil \frac{n}{4} \cdot \frac{n - 3}{n - \frac{10}{4}} \right\rceil - \left\lceil \frac{n}{4} \right\rceil \leq 0$$

We next prove that  $\lceil \frac{n^2 - 3n + 2}{4n - 10} \rceil - \lceil \frac{n}{4} \rceil \geq 0$  holds.

$$\left\lceil \frac{n^2 - 3n + 2}{4n - 10} \right\rceil - \left\lceil \frac{n}{4} \right\rceil \geq \left\lceil \frac{n}{4} \cdot \frac{n + \frac{2}{5}}{n - \frac{5}{2}} \right\rceil - \left\lceil \frac{n}{4} \right\rceil \geq 0$$

Hence, the proof is completed.  $\square$

For rique layouts, the analog of Lemma 2 is the following, which has been used to show a lower bound of  $(1 - \frac{\sqrt{2}}{2})(n - 2)$  on the rique-number of  $K_n$  [4].

**Lemma 4** (Bekos et al. [4]). *A graph with  $n$  vertices admitting a rique layout with  $k$  pages has at most  $(2n + 2)k - k^2 + (n - 3)$  edges.*

In the next theorem, we improve the best-known upper bound on the rique-number of  $K_n$  from  $\lceil \frac{n}{3} \rceil$  [4] to  $\lfloor \frac{n-1}{3} \rfloor$ .

**Theorem 5.** *The rique-number of  $K_n$  is at most  $\lfloor \frac{n-1}{3} \rfloor$ .*

*Proof.* For our proof, we distinguish three cases, namely,  $n \bmod 3 \in \{0, 1, 2\}$ . We describe each of these cases separately in the following.

**Case 1:**  $n \bmod 3 = 0$ . We start our proof assuming  $n \bmod 3 = 0$  and we prove that  $K_n$  admits a rique layout  $\mathcal{L}$  with  $\frac{n}{3} - 1$  riques. Our construction contains seven “special” pages, namely, the ones in  $\{1, 2, 3, 4, \frac{n}{3} - 3, \frac{n}{3} - 2, \frac{n}{3} - 1\}$ ; blue, red, green, dark-purple, gray, light-purple and yellow in Fig. 9a. The remaining pages of  $\mathcal{L}$  are uniform.

Page 1 of  $\mathcal{L}$  contains the following  $2n$  edges; see Fig. 2:

- $\{(v_1, v_j), j = 2, \dots, n\}_{ht}$ ; dark red in Fig. 2,
- $\{(v_i, v_n), i = 2, \dots, \frac{n}{3}\}_{ht}$ ; red in Fig. 2,
- $\{(v_{\frac{n}{3}}, v_j), j = \frac{n}{3} + 1, \dots, \frac{2n}{3} + 1\}_{hh}$ ; light red in Fig. 2,
- $\{(v_{\frac{2n}{3}+1}, v_j), j = \frac{2n}{3} + 2, \dots, n\}_{hh}$ ; blue in Fig. 2,
- $\{(v_{n-1}, v_n)\}_{hh}$ ; light blue in Fig. 2 .

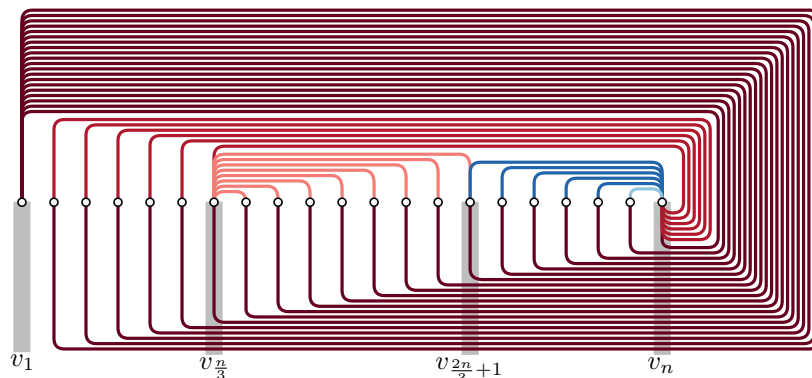


Figure 2: Page 1 of  $\mathcal{L}$  when  $n \bmod 3 = 0$ .

Page 2 of  $\mathcal{L}$  contains the following  $2n - 7$  edges:

- $\{(v_2, v_j), j = 3, \dots, n - 1\}_{ht}$ ; dark red in Fig. 3,
- $\{(v_i, v_{n-1}), i = 3, \dots, \frac{n}{3} + 1\}_{ht}$ ; red in Fig. 3,
- $\{(v_{\frac{n}{3}+1}, v_n)\}_{ht}$ ; orange in Fig. 3,
- $\{(v_{\frac{n}{3}+1}, v_j), j = \frac{n}{3} + 2, \dots, \frac{2n}{3}\}_{hh}$ ; blue in Fig. 3,
- $\{(v_{\frac{2n}{3}}, v_j), j = \frac{2n}{3} + 1, \dots, n\}_{hh}$ ; light blue in Fig. 3.

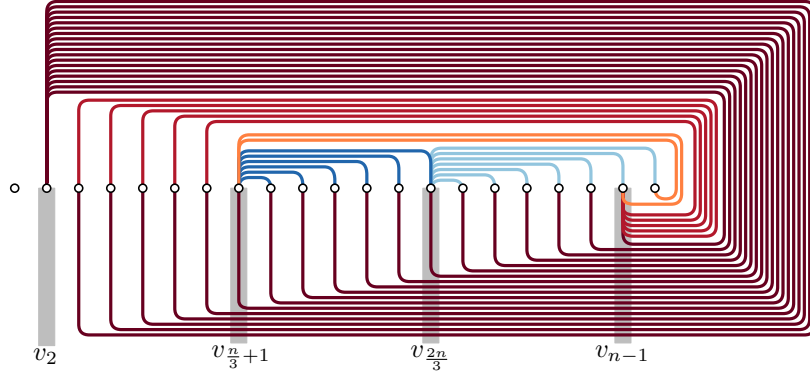


Figure 3: Page 2 of  $\mathcal{L}$  when  $n \bmod 3 = 0$ .

Page 3 of  $\mathcal{L}$  contains the following  $2n - 5$  edges:

- $\{(v_3, v_j), j = 4, \dots, n - 2\}_{ht}$ ; dark red in Fig. 4,
- $\{(v_i, v_{n-2}), i = 4, \dots, \frac{n}{3} + 1\}_{ht}$ ; red in Fig. 4,
- $\{(v_{\frac{2n}{3}+2}, v_j), j = n - 2, \dots, n\}_{ht}$ ; orange in Fig. 4,
- $\{(v_{\frac{n}{3}+1}, v_{\frac{2n}{3}+1})\}_{hh}$ ; blue in Fig. 4,
- $\{(v_{\frac{n}{3}+2}, v_j), j = \frac{2n}{3} - 1, \frac{2n}{3}, \frac{2n}{3} + 1\}_{hh}$ ; light blue in Fig. 4,
- $\{(v_{\frac{n}{3}+3}, v_j), j = \frac{n}{3} + 4, \dots, \frac{2n}{3} - 1\}_{hh}$ ; pink in Fig. 4,
- $\{(v_{\frac{2n}{3}+2}, v_j), j = \frac{2n}{3} + 3, \dots, n - 3\}_{hh}$ ; light red in Fig. 4,
- $\{(v_{n-3}, v_j), j = n - 2, n - 1, n\}_{hh}$ ; light orange in Fig. 4.

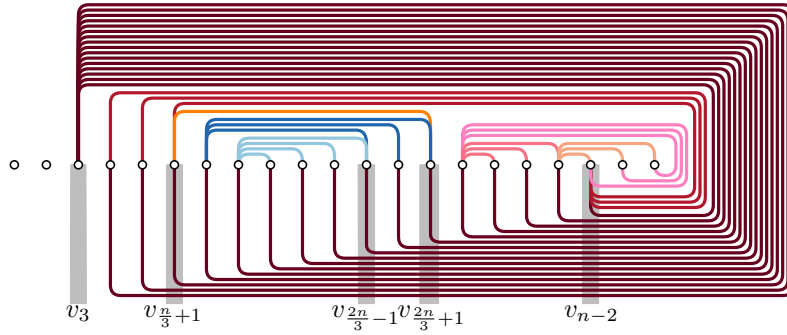


Figure 4: Page 3 of  $\mathcal{L}$  when  $n \bmod 3 = 0$ .

For  $p = 4, \dots, \frac{n}{3} - 4$ , page  $p$  of  $\mathcal{L}$  contains the following  $\frac{n}{3} - 2p + 3$  edges:

- $\{(v_p, v_j), j = p + 1, \dots, n - p + 1\}_{ht}$ ; dark red in Fig. 5,
- $\{(v_i, v_j), i = p + 1, \dots, \frac{n}{3} + 1, j = n - p + 1\}_{ht}$ ; red in Fig. 5,
- $\{(v_i, v_j), i = \frac{n}{3} + (p + 1), j = n - p + 1, \dots, n\}_{ht}$ ; pink in Fig. 5,
- $\{(v_i, v_j), i = \frac{n}{3} + (p + 1), j = \frac{2n}{3} + (p - 2), \dots, n - p\}_{hh}$ ; blue in Fig. 5,

- $\{(v_i, v_j), i = n - p + 1, j = n - p, \dots, n\}_{hh}$ ; light blue in Fig. 5,
- $\{(v_i, v_j), i = \frac{n}{3} + (p + 2), j = \frac{n}{3} + (p + 3), \dots, \frac{2n}{3} + (p - 2)\}_{hh}$ ; orange in Fig. 5.

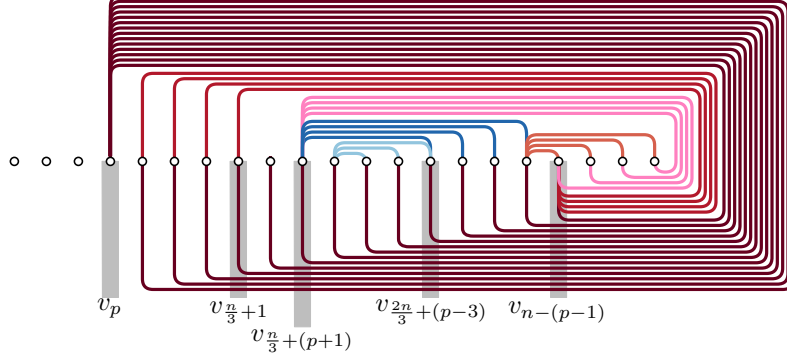


Figure 5: Page  $p = 4, \dots, \frac{n}{3} - 4$  of  $\mathcal{L}$  when  $n \bmod 3 = 0$ .

Page  $\frac{n}{3} - 3$  of  $\mathcal{L}$  contains the following  $\frac{4n}{3} + 6$  edges:

- $\{(v_{\frac{n}{3}-3}, v_j), j = \frac{n}{3} - 2, \dots, \frac{2n}{3} + 4\}_{ht}$ ; dark red in Fig. 6,
- $\{(v_i, v_{\frac{2n}{3}+4}), i = \frac{n}{3} - 2, \dots, \frac{n}{3} + 1\}_{ht}$ ; red in Fig. 6,
- $\{(v_{\frac{n}{3}+3}, v_j), j = \frac{2n}{3} + 4, \dots, n - 1\}_{ht}$ ; light blue in Fig. 6,
- $\{(v_{\frac{2n}{3}+3}, v_j), j = n - 1, n\}_{ht}$ ; pink in Fig. 6,
- $\{(v_{\frac{n}{3}+3}, v_j), j = \frac{2n}{3}, \dots, \frac{2n}{3} + 3\}_{hh}$ ; dark blue in Fig. 6,
- $\{(v_{\frac{n}{3}+4}, v_j), j = \frac{n}{3} + 5, \dots, \frac{2n}{3}\}_{hh}$ ; orange in Fig. 6,
- $\{(v_{\frac{2n}{3}+3}, v_j), j = \frac{2n}{3} + 3, \dots, n - 2\}_{hh}$ ; red in Fig. 6,
- $\{(v_{n-2}, v_j), j = n - 1, n\}_{hh}$ ; dark orange in Fig. 6.

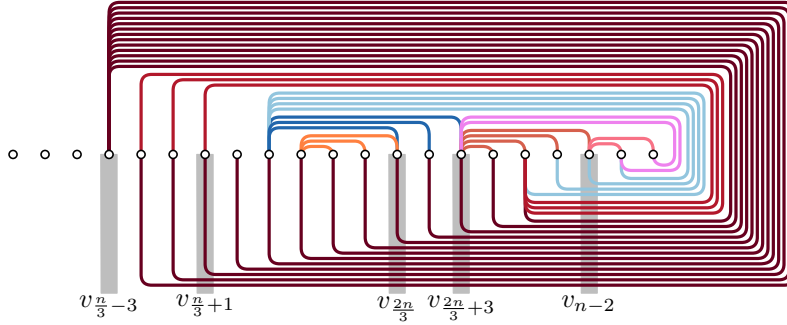


Figure 6: Page  $\frac{n}{3} - 3$  of  $\mathcal{L}$  when  $n \bmod 3 = 0$ .

Page  $\frac{n}{3} - 2$  of  $\mathcal{L}$  contains the following  $\frac{4n}{3} + 3$  edges:

- $\{(v_{\frac{n}{3}-2}, v_j), j = \frac{n}{3} - 1, \dots, \frac{2n}{3} + 3\}_{ht}$ ; dark red in Fig. 7,
- $\{(v_i, v_{\frac{2n}{3}+3}), i = \frac{n}{3} - 1, \dots, \frac{n}{3} + 1\}_{ht}$ ; red in Fig. 7,

- $\{(v_{\frac{n}{3}+2}, v_j), j = \frac{2n}{3} + 3, \dots, n\}_{ht}$ ; light red in Fig. 7,
- $\{(v_{\frac{n}{3}+3}, v_n)_{ht}$ ; pink in Fig. 7,
- $\{(v_{\frac{n}{3}+4}, v_j), j = \frac{2n}{3} + 1, \dots, n\}_{hh}$ ; dark orange in Fig. 7,
- $\{(v_{\frac{n}{3}+5}, v_j), j = \frac{n}{3} + 6, \dots, \frac{2n}{3} + 1\}_{hh}$ ; orange in Fig. 7.

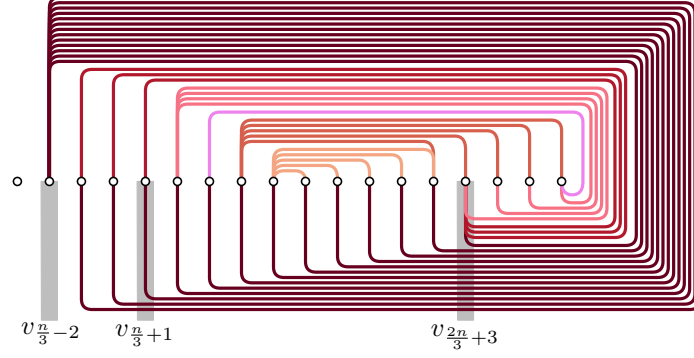


Figure 7: Page  $\frac{n}{3} - 2$  of  $\mathcal{L}$  when  $n \bmod 3 = 0$ .

Page  $\frac{n}{3} - 1$  of  $\mathcal{L}$  contains the following  $n + 9$  edges:

- $\{(v_{\frac{n}{3}-1}, v_j), j = \frac{n}{3}, \dots, \frac{2n}{3} + 2\}_{ht}$ ; dark red in Fig. 8,
- $\{(v_i, v_{\frac{2n}{3}+2}), i = \frac{n}{3}, \dots, \frac{n}{3} + 2\}_{ht}$ ; red in Fig. 8,
- $\{(v_{\frac{2n}{3}-2}, v_j), j = n - 5, \dots, n\}_{ht}$ ; light red in Fig. 8,
- $\{(v_{\frac{n}{3}+2}, v_j), j = \frac{n}{3} + 3, \dots, \frac{2n}{3} - 2\}_{hh}$ ; orange in Fig. 8,
- $\{(v_{\frac{2n}{3}-1}, v_j), j = \frac{2n}{3}, \dots, n\}_{hh}$ ; light orange in Fig. 8.

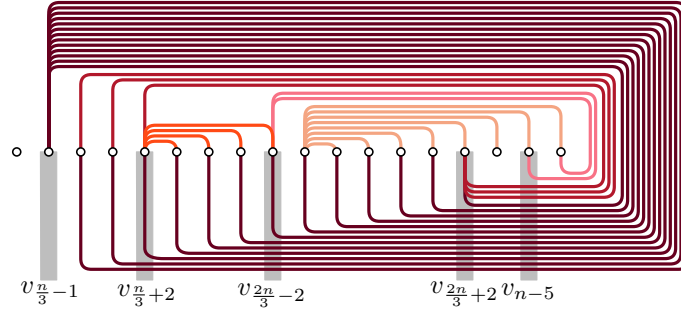


Figure 8: Page  $\frac{n}{3} - 1$  of  $\mathcal{L}$  when  $n \bmod 3 = 0$ .

So, in total  $\mathcal{L}$  has  $(2n - 1) + (2n - 6) + (2n - 4) + (\frac{5n}{3} - 5) + \sum_{p=5}^{\frac{n}{3}-4} (\frac{5n}{3} - p + 1) + (n + 14) + (\frac{4n}{3} + 3) + (\frac{4n}{3} + 3) = \frac{n(n-1)}{2}$  edges. Since no two edges have been assigned to the same rique and all edges in the same rique form a cylindric layout, it follows that the rique number of  $K_n$  is at most  $\lfloor \frac{n-1}{3} \rfloor$  when  $n \bmod 3 = 0$ .



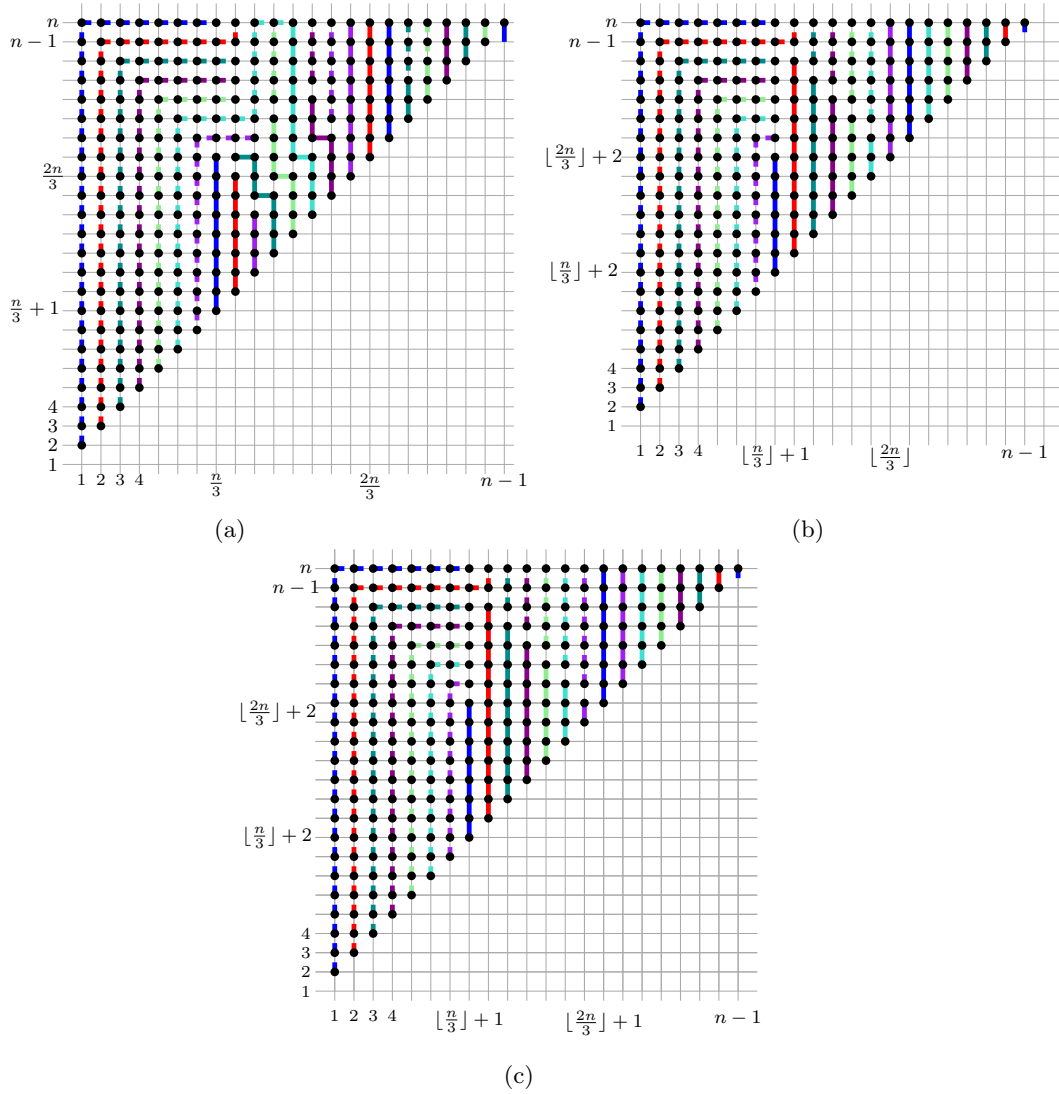


Figure 9: Illustration of the grid representation of a rique layout of  $K_n$  with (a)  $n \bmod 3 = 0$  (b)  $n \bmod 3 = 1$ , and (c)  $n \bmod 3 = 2$ , in which paths of the same color correspond to the same rique. The points of the grid that are covered by a solid (dashed) path are head-head (head-tail, respectively).

**Case 2:**  $n \bmod 3 = 1$ . In this case, we show that the  $K_n$  admits a riqe layout with  $\lfloor \frac{n}{3} \rfloor$  riques. As in Case 1, our construction contains again “special” pages, namely, the ones in  $\{1, 2, \lfloor \frac{n-1}{3} \rfloor\}$ ; blue, red and purple in Fig. 9b. The remaining pages of  $\mathcal{L}$  are uniform.

Page 1 of  $\mathcal{L}$  contains the following  $2n - 1$  edges:

- $\{(u_1, v_j), j = 2, \dots, n\}_{ht}$ ; dark red in Fig. 10,
- $\{(u_i, v_n), i = 2, \dots, \frac{n-1}{3} + 1\}_{ht}$ ; red in Fig. 10,
- $\{(u_{\frac{n-1}{3}+1}, v_j), j = \frac{n-1}{3} + 2, \dots, \frac{2n-2}{3} + 1\}_{hh}$ ; light red in Fig. 10,
- $\{(u_{\frac{2n-2}{3}+1}, v_j), j = \frac{2n-2}{3} + 2, \dots, n\}_{hh}$ ; blue in Fig. 10,
- $\{(u_{n-1}, v_n)\}_{hh}$ ; light blue in Fig. 10.

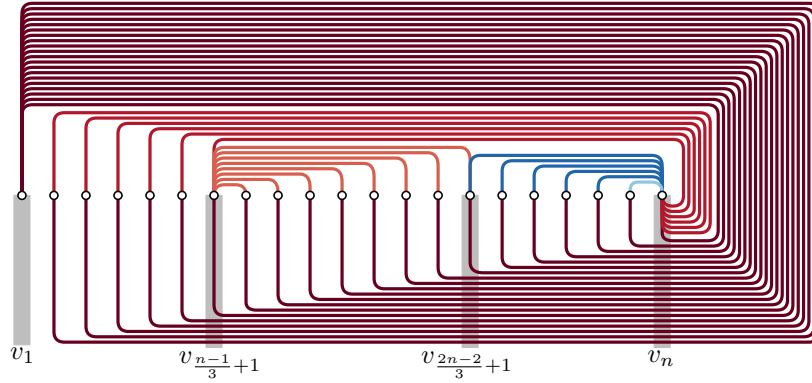


Figure 10: Page 1 of  $\mathcal{L}$  when  $n \bmod 3 = 1$ .

Page 2 of  $\mathcal{L}$  contains the following  $2n - 4$  edges:

- $\{(u_2, v_j), j = 3, \dots, n-1\}_{ht}$ ; dark red in Fig. 11,
- $\{(u_i, v_{n-1}), i = 3, \dots, \frac{n-1}{3} + 1\}_{ht}$ ; red in Fig. 11,
- $\{(u_{\frac{n-1}{3}+2}, v_j), j = n-1, n\}_{ht}$ ; light red in Fig. 11,

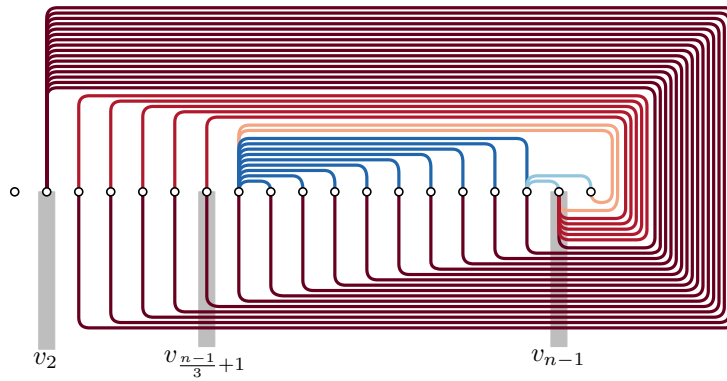


Figure 11: Page 2 of  $\mathcal{L}$  when  $n \bmod 3 = 1$ .

- $\{(u_{\frac{n-1}{3}+2}, v_j), j = \frac{n-1}{3} + 3, \dots, n-2\}_{hh}$ ; blue in Fig. 11,
- $\{(u_{n-2}, v_j), j = n-1, n\}_{hh}$ ; light blue in Fig. 11.

For  $p = 3, \dots, \frac{n-1}{3} - 1$ , page  $p$  of  $\mathcal{L}$  contains the following  $2n - 3p + 2$  edges:

- $\{(u_p, v_j), j = p+1, \dots, n-p+1\}_{ht}$ ; dark red in Fig. 12,
- $\{(u_i, v_{n-p+1}), i = p+1, \dots, \frac{n-1}{3} + 1\}_{ht}$ ; red in Fig. 12,
- $\{(u_{\frac{n-1}{3}+p}, v_j), j = n-p+1, \dots, n\}_{ht}$ ; orange in Fig. 12,
- $\{(u_{\frac{n-1}{3}+p}, v_j), j = \frac{n-1}{3} + (p+1), \dots, n-p\}_{hh}$ ; blue in Fig. 12,
- $\{(u_{n-p}, v_j), j = n-p+1, \dots, n\}_{hh}$ ; light blue in Fig. 12.

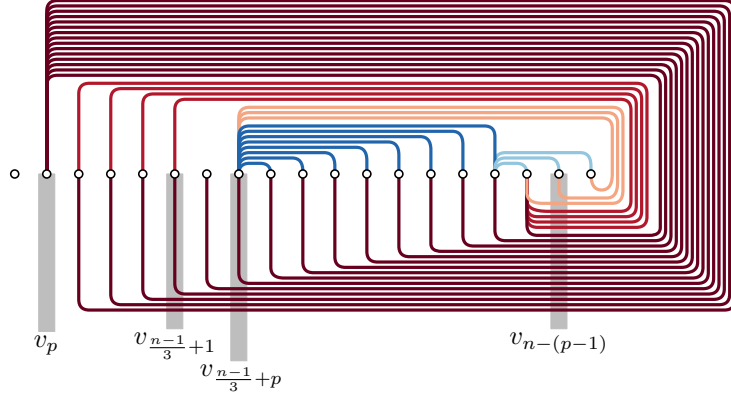


Figure 12: Page  $p = 3, \dots, \frac{n-1}{3} - 1$  of  $\mathcal{L}$  when  $n \bmod 3 = 1$ .

Page  $\lfloor \frac{n-1}{3} \rfloor$  of  $\mathcal{L}$  contains the following  $2(\frac{n-1}{3}) + 4$  edges:

- $\{(u_{\frac{n-1}{3}}, v_j), j = \frac{n-1}{3} + 1, \dots, \frac{2n-2}{3} + 2\}_{ht}$ ; dark red in Fig. 13,
- $\{(u_{\frac{n-1}{3}+1}, v_{\frac{2n-2}{3}+2})\}_{ht}$ ; red in Fig. 13,
- $\{(u_{\frac{2n-2}{3}}, v_j), j = \frac{2n-2}{3} + 1, \dots, n\}_{hh}$ ; orange in Fig. 13.

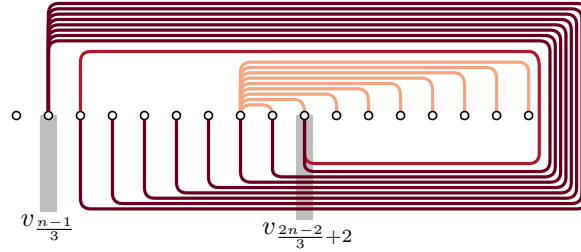


Figure 13: Page  $\lfloor \frac{n-1}{3} \rfloor$  of  $\mathcal{L}$  when  $n \bmod 3 = 1$ .

So, when  $n \bmod 3 = 1$ ,  $\mathcal{L}$  has  $2n - 1 + 2n - 4 + \sum_{p=3}^{\frac{n-1}{3}-1} (2n - 3p + 2) + 2(\frac{n-1}{3}) + 4 = \frac{n(n-1)}{2}$  edges. Since no two edges have been assigned to the same rique and all edges in the same rique form a cylindrical layout, it follows that the rique number of  $K_n$  is at most  $\lfloor \frac{n-1}{3} \rfloor$  when  $n \bmod 3 = 1$ .

**Case 3:**  $n \bmod 3 = 2$ . We continue with the case  $n \bmod 3 = 2$ . In this case, we show that the  $K_n$  admits a riqe layout with  $\lfloor \frac{n}{3} \rfloor$  riques. As with the previous two cases, our construction contains again “special” pages, namely, the ones in  $\{1, 2\}$ ; blue and red in Fig. 9c. The remaining pages of  $\mathcal{L}$  are uniform.

Page 1 of  $\mathcal{L}$  contains the following  $2n$  edges:

- $\{(u_1, v_j), j = 2, \dots, n\}_{ht}$ ; dark red in Fig. 14,
- $\{(u_i, v_n), i = 2, \dots, \frac{n-2}{3} + 1\}_{ht}$ ; red in Fig. 14,
- $\{(u_{\frac{n-2}{3}+1}, v_j), j = \frac{n-2}{3} + 2, \dots, \frac{2n-4}{3} + 2\}_{hh}$ ; light red in Fig. 14,
- $\{(u_{\frac{2n-4}{3}+2}, v_j), j = \frac{2n-4}{3} + 3, \dots, n\}_{hh}$ ; blue in Fig. 14,
- $\{(u_{n-1}, v_n)\}_{hh}$ ; light blue in Fig. 14.

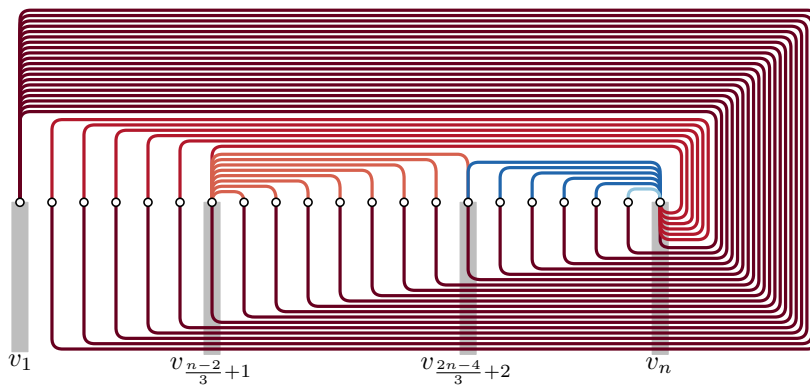


Figure 14: Page 1 of  $\mathcal{L}$  when  $n \bmod 3 = 2$ .

Page 2 of  $\mathcal{L}$  contains the following  $2n - 4$  edges:

- $\{(u_2, v_j), j = 3, \dots, n - 1\}_{ht}$ ; dark red in Fig. 15,
- $\{(u_i, v_{n-1}), i = 3, \dots, \frac{n-2}{3} + 2\}_{ht}$ ; red in Fig. 15,

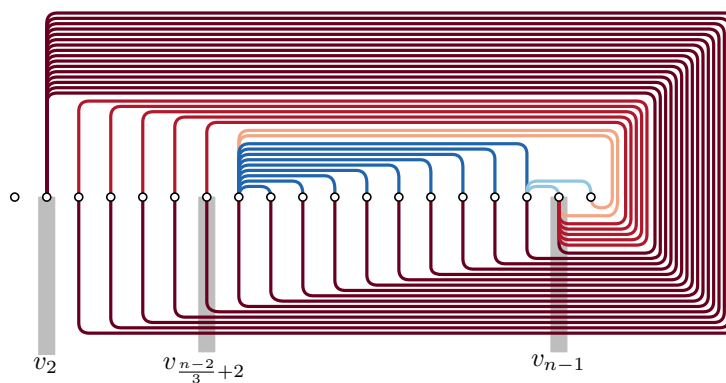


Figure 15: Page 2 of  $\mathcal{L}$  when  $n \bmod 3 = 2$ .

- $\{(u_{\frac{n-2}{3}+2}, v_j), j = n-1, n\}_{ht}$ ; light red in Fig. 15,
- $\{(u_{\frac{n-2}{3}+2}, v_j), j = \frac{n-2}{3} + 3 \dots, n-2\}_{hh}$ ; blue in Fig. 15,
- $\{(u_{n-2}, v_j), j = n-1, n\}_{hh}$ ; light blue in Fig. 15.

For  $p = 3, \dots, \frac{n-2}{3}$ , page  $p$  of  $\mathcal{L}$  contains the following  $2n - 3p + 2$  edges:

- $\{(u_p, v_j), j = p+1, \dots, n-p+1\}_{ht}$ ; dark red in Fig. 16,
- $\{(u_i, v_{n-p+1}), i = p+1, \dots, \frac{n-2}{3} + 1\}_{ht}$ ; red in Fig. 16,
- $\{(u_{\frac{n-2}{3}+p}, v_j), j = n-p+1, \dots, n\}_{ht}$ ; light red in Fig. 16,
- $\{(u_{\frac{n-2}{3}+p}, v_j), j = \frac{n-2}{3} + (p+1), \dots, n-p\}_{hh}$ ; blue in Fig. 16,
- $\{(u_{n-p}, v_j), j = n-p+1, \dots, n\}_{hh}$ ; light blue in Fig. 16.

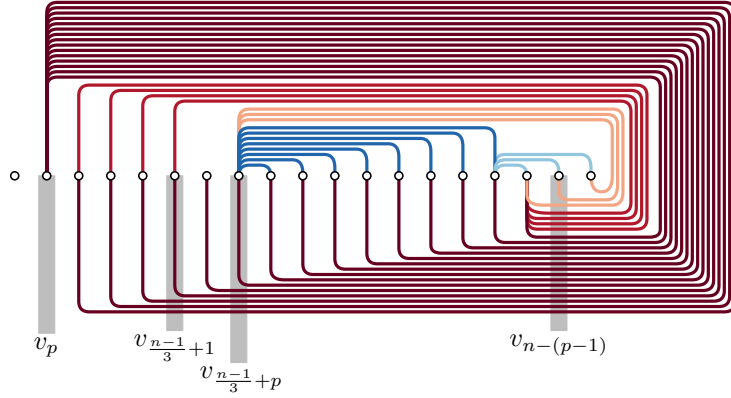


Figure 16: Page  $p = 3, \dots, \frac{n-2}{3}$  of  $\mathcal{L}$  when  $n \bmod 3 = 2$ .

So, in total  $\mathcal{L}$  has  $2n + 2n - 4 + \sum_{p=3}^{\frac{n-2}{3}} (2n - 3p + 2) = \frac{n(n-1)}{2}$  edges. Since no two edges have been assigned to the same rique and all edges in the same rique form a cylindric layout, it follows that the rique number of  $K_n$  is at most  $\lfloor \frac{n-1}{3} \rfloor$  when  $n \bmod 3 = 2$ .  $\square$

**Remark 1.** Using the SAT formulation that we present in Section 5 we were able to show that the upper bound of Theorem 5 is tight for all values of  $n \leq 30$ . However, we were not able to show a matching lower bound. In view of these observations, we conjecture in Section 6 that the rique-number of  $K_n$  is exactly  $\lfloor \frac{n-1}{3} \rfloor$ .

## 4 Complete bipartite graphs

In this section, we study the deque- and rique-numbers of the complete bipartite graph  $K_{n,n}$ . Let the two parts of  $K_{n,n}$  be  $A = \{a_1, \dots, a_n\}$  and  $B = \{b_1, \dots, b_n\}$  with  $|A| = |B| = n$ . W.l.o.g., we may assume that in the computed layouts  $a_1 \prec \dots \prec a_n$  and  $b_1 \prec \dots \prec b_n$  holds.

**Theorem 6.** *The deque-number of  $K_{n,n}$  is at most  $\lceil \frac{n}{3} \rceil$ .*

*Proof.* Assume that  $n \bmod 3 = 0$ ; the remaining cases follow from this one. We describe a deque layout  $\mathcal{L}$  of  $K_{n,n}$  with  $\frac{n}{3}$  dequeues, in which the underlying order is:  $a_1 \prec \dots \prec a_{n/3} \prec b_1 \dots \prec b_{2n/3} \prec a_{n/3+1} \prec \dots \prec a_n \prec b_{2n/3+1} \prec \dots \prec b_n$ ; for an illustration of the corresponding matrix representation refer to Fig. 26 and observe that it consists of four blocks, e.g., the middle block corresponds to the edges between  $a_{n/3+1}, \dots, a_n$  and  $b_1, \dots, b_{2n/3}$ .

Page 1 of  $\mathcal{L}$  contains the following  $2n + 16$  edges:

- $\{(a_1, b_j), j = \frac{2n}{3} + 4, \dots, n\}_{hh}$ ; dark red in Fig. 17,
- $\{(a_1, b_6)\}_{hh}$ ; red in Fig. 17,
- $\{(a_2, b_j), j = 1, \dots, 6\}_{hh}$ ; light red in Fig. 17,
- $\{(a_{\frac{n}{3}+8}, b_j), j = 8, 9, 10\}_{hh}$ ; orange in Fig. 17,
- $\{(a_i, b_{10}), i = \frac{n}{3} + 1, \dots, \frac{n}{3} + 7\}_{hh}$ ; light orange in Fig. 17,
- $\{(a_i, b_{\frac{2n}{3}+4}), i = \frac{n}{3} + 8, \dots, n\}_{hh}$ ; green in Fig. 17,
- $\{(a_2, b_j), j = n - 2, \dots, n\}_{tt}$ ; dark blue in Fig. 17,
- $\{(a_i, b_{\frac{2n}{3}+5}), i = \frac{n}{3} - 2, \dots, \frac{n}{3}\}_{tt}$ ; blue in Fig. 17,
- $\{(a_{\frac{n}{3}}, b_j), j = \frac{2n}{3} + 1, \frac{2n}{3} + 2\}_{tt}$ ; light blue in Fig. 17.
- $\{(a_n, b_1), (a_n, b_2), (a_{n-1}, b_2)\}_{tt}$ ; pink in Fig. 17,
- $\{(a_i, b_j), (a_{i-1}, b_j), i = n - 1, \dots, \frac{2n}{3} + 3, j = 4, \dots, \frac{n}{3}\}_{tt}$ ; light pink in Fig. 17,
- $\{(a_i, b_{\frac{n}{3}}), i = \frac{2n}{3} + 1, \frac{2n}{3} + 2\}_{tt}$ ; dark orange in Fig. 17,
- $\{(a_{\frac{2n}{3}+1}, b_j), j = \frac{n}{3} + 1, \dots, \frac{n}{3} + 3\}_{tt}$ ; dark green in Fig. 17,
- $\{(a_i, b_{\frac{n}{3}+3}), i = \frac{n}{3} + 1, \dots, \frac{2n}{3}\}_{tt}$ ; green in Fig. 17.

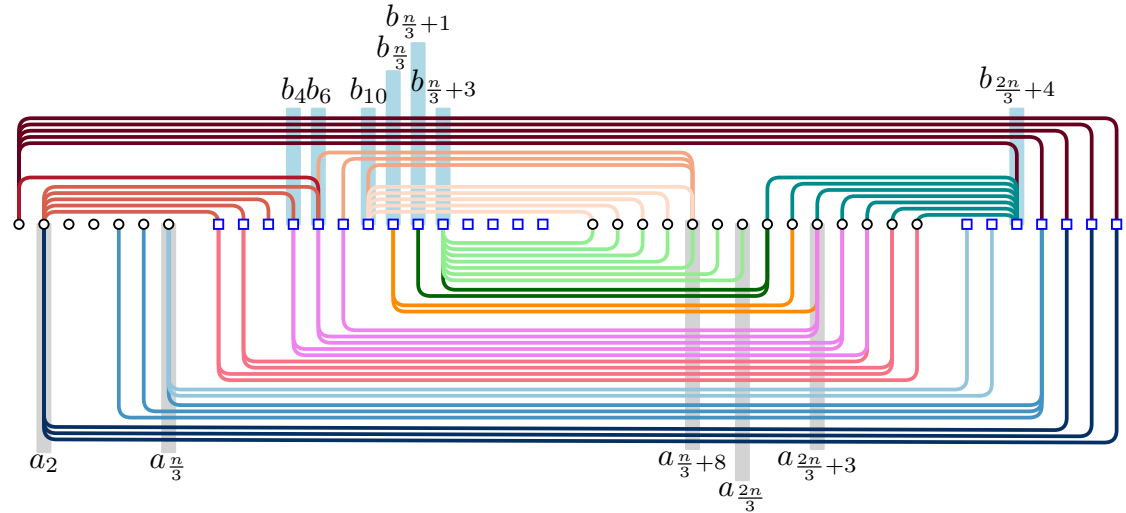


Figure 17: Page 1 of  $\mathcal{L}$ .

Page 2 of  $\mathcal{L}$  contains the following  $\frac{8n}{3} + 5$  edges:

- $\{(a_1, b_{\frac{2n}{3}+3})\}_{ht}$ ; black in Fig. 18,
- $\{(a_2, b_j), j = \frac{2n}{3} + 3, \dots, n - 3\}_{ht}$ ; dark red in Fig. 18,
- $\{(a_3, b_j), j = n - 3, \dots, n - 1\}_{ht}$ ; red in Fig. 18,
- $\{(a_i, b_n), i = 3, \dots, \frac{n}{3}\}_{ht}$ ; dark orange in Fig. 18,
- $\{(a_i, b_1), i = n - 3, n - 4\}_{hh}$ ; light orange in Fig. 18,
- $\{(a_i, b_2), i = n - 4, n - 5\}_{hh}$ ; dark orange in Fig. 18,
- $\{(a_i, b_j), (a_{i-1}, b_j), i = n - 5, \dots, \frac{2n}{3} + 1, j = 4, \dots, \frac{n}{3} - 2\}_{hh}$ ; dark pink in Fig. 18,
- $\{(a_i, b_{\frac{n}{3}-2}), i = \frac{2n}{3} + 1, \dots, \frac{2n}{3} - 1\}_{hh}$ ; light pink in Fig. 18,
- $\{(a_{\frac{2n}{3}-1}, b_j), j = \frac{n}{3} - 1, \frac{n}{3}\}_{hh}$ ; light gray in Fig. 18,
- $\{(a_i, b_{\frac{n}{3}+1}), i = \frac{n}{3} + 1, \dots, \frac{2n}{3} - 1\}_{hh}$ ; gray in Fig. 18,
- $\{(a_i, b_n), i = n - 3, \dots, n\}_{hh}$ ; pink in Fig. 18,
- $\{(a_1, b_i), i = 1, \dots, 5\}_{tt}$ ; light green in Fig. 18,
- $\{(a_i, b_j), (a_i, b_{j+1}), i = n - 1, \dots, \frac{2n}{3} + 4, j = 5, \dots, \frac{n}{3}\}_{tt}$ ; green in Fig. 18,
- $\{(a_i, b_{\frac{n}{3}+1}), i = \frac{2n}{3} + 2, \frac{2n}{3} + 3\}_{tt}$ ; dark blue in Fig. 18,
- $\{(a_{\frac{2n}{3}+2}, b_j), i = \frac{n}{3} + 2, \frac{n}{3} + 3\}_{tt}$ ; blue in Fig. 18,
- $\{(a_i, b_{\frac{n}{3}+4}), i = \frac{n}{3} + 1, \dots, \frac{2n}{3} + 2\}_{tt}$ ; light blue in Fig. 18.

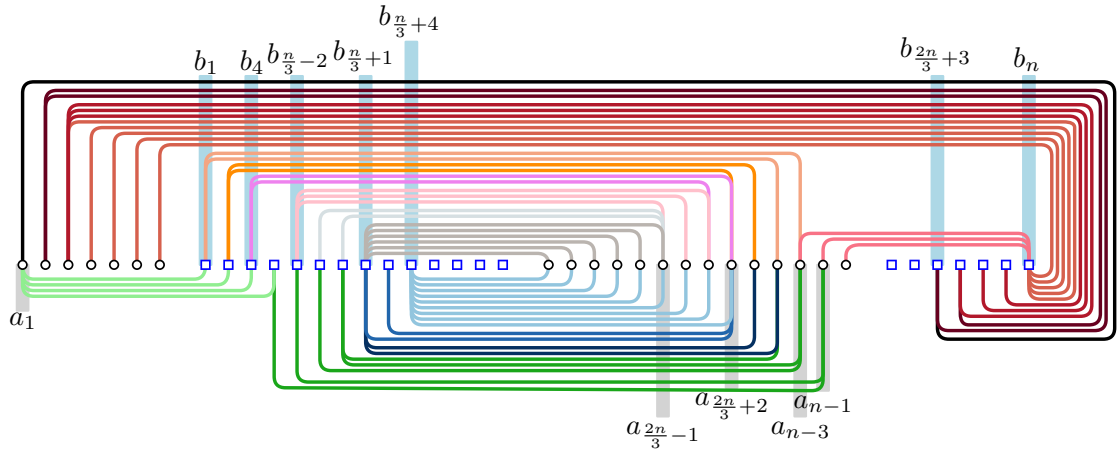


Figure 18: Page 2 of  $\mathcal{L}$ .

Page  $p = 3, 4$  of  $\mathcal{L}$  contains the following  $\frac{8n}{3} + p + 5$  edges:

- $\{(a_i, b_{2p+1}), i = 1, \dots, p-1\}_{tt}$ ; green in Fig. 19,
- $\{(a_p, b_j), j = 1, \dots, 2p+1\}_{tt}$ ; dark green in Fig. 19,
- $\{(a_i, b_{\frac{2n}{3}+5-p}), i = 1, \dots, p-1\}_{ht}$ ; dark red in Fig. 19,
- $\{(a_p, b_j), j = \frac{2n}{3} + 5 - p, \dots, n-1-p\}_{ht}$ ; red in Fig. 19,
- $\{(a_{p+1}, b_j), j = n-1-p, \dots, n+1-p\}_{ht}$ ; pink in Fig. 19,
- $\{(a_i, b_{n+2-p}), i = 1+p, \dots, \frac{n}{3}\}_{ht}$ ; light pink in Fig. 19,
- $\{(a_i, b_1), i = n-2p+1, n-2p\}_{hh}$ ; purple in Fig. 19,
- $\{(a_i, b_2), i = n-2p, n-2p-1\}_{hh}$ ; orange in Fig. 19,
- $\{(a_i, b_j), (a_{i-1}, b_j), i = n-2p-1, \dots, \frac{2n}{3} + 4 - p, j = 4, \dots, \frac{n}{3} - p - 1\}_{hh}$ ; yellow in Fig. 19,
- $\{(a_i, b_{\frac{n}{3}-p}), i = \frac{2n}{3} - p + 3, \dots, \frac{2n}{3} - p + 1\}_{hh}$ ; dark pink in Fig. 19,
- $\{(a_{\frac{2n}{3}-p}, b_j), j = \frac{n}{3} - p + 1, \frac{n}{3} - p + 2\}_{hh}$ ; light yellow in Fig. 19,
- $\{(a_i, b_{\frac{n}{3}-p+3}), i = \frac{n}{3} + 1, \dots, \frac{2n}{3} - p + 1\}_{hh}$ ; dark yellow in Fig. 19,
- $\{(a_i, b_j), (a_i, b_{j+1}), i = n-1, \dots, \frac{2n}{3} + p + 2, j = 5, \dots, \frac{n}{3} + p - 2\}_{tt}$ ; light green in Fig. 19,
- $\{(a_i, b_{\frac{2n}{3}+p-1}), i = \frac{2n}{3} + p, \frac{2n}{3} + p + 1\}_{tt}$ ; blue in Fig. 19,
- $\{(a_{\frac{2n}{3}+p}, b_j), i = \frac{n}{3} + p, \frac{n}{3} + p + 1\}_{tt}$ ; dark blue in Fig. 19,
- $\{(a_i, b_{\frac{n}{3}+p+2}), i = \frac{n}{3} + 1, \dots, \frac{2n}{3} + p\}_{tt}$ ; light blue in Fig. 19,
- $\{(a_{n+2-2p}, b_j), j = n+2-p, \dots, n\}_{hh}$ ; light gray in Fig. 19,
- $\{(a_i, b_{n+2-p}), i = n+3-2p, \dots, n\}_{hh}$ ; gray in Fig. 19,
- $\{(a_{n+1-2p}, b_j), j = n+2-p, \dots, n\}_{ht}$ ; black in Fig. 19.

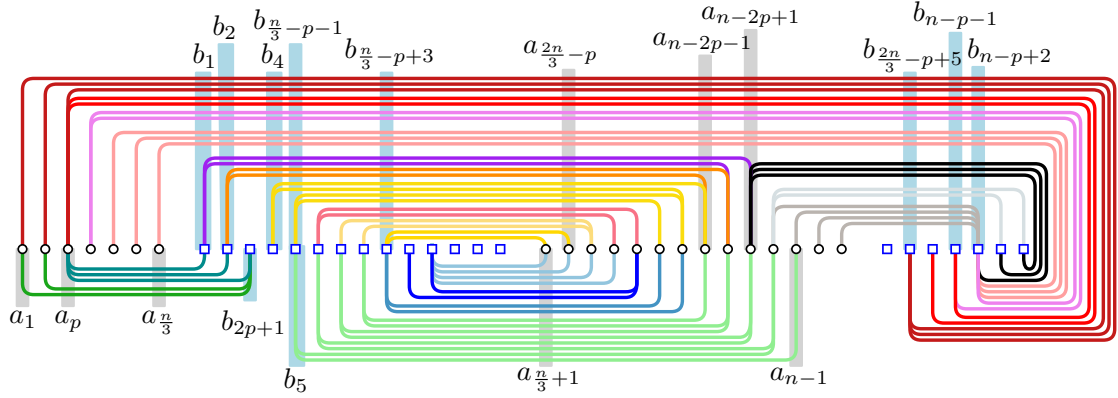


Figure 19: Page  $p = 3, 4$  of  $\mathcal{L}$ .





For  $p = \frac{n}{3} - 7, \dots, \frac{n}{3} - 4$ , page  $p$  of  $\mathcal{L}$  contains  $\frac{8n}{3} - 2p - 1$  edges:

- $\{(a_i, b_1), i = n - 2p + 1, n - 2p\}_{hh}$ ; purple in Fig. 21,
- $\{(a_i, b_2), i = n - 2p, n - 2p - 1\}_{hh}$ ; dark orange in Fig. 21,
- $\{(a_i, b_j), (a_{i-1}, b_j), i = n - 2p - 1, \dots, n - 2p + 3, j = 4, \dots, 6\}_{hh}$ ; yellow in Fig. 21,
- $\{(a_i, b_{\frac{n}{3}-p}), i = \frac{2n}{3} - p + 1, \dots, \frac{2n}{3} - p + 3\}_{hh}$ ; dark pink in Fig. 21,
- $\{(a_{\frac{2n}{3}-p}, b_j), j = \frac{n}{3} - p, \frac{n}{3} - p + 1\}_{hh}$ ; light orange in Fig. 21,
- $\{(a_i, b_{\frac{n}{3}-p+2}), i = \frac{n}{3} + 1, \dots, \frac{2n}{3} - p\}_{hh}$ ; orange in Fig. 21,
- $\{(a_i, b_j), (a_i, b_{j+1}), i = n - 1, \dots, n - 5, j = 2p, \dots, \frac{n}{3} + p - 2\}_{tt}$ ; light green in Fig. 21,
- $\{(a_i, b_{\frac{n}{3}+p+2}), i = \frac{n}{3} + 1, \dots, \frac{2n}{3} + p\}_{tt}$ ; light blue in Fig. 21,
- $\{(a_{\frac{2n}{3}+p}, b_j), j = \frac{n}{3} + p - 1, \dots, \frac{n}{3} + p + 1\}_{tt}$ ; blue in Fig. 21,
- $\{(a_{\frac{2n}{3}+p+1}, b_{\frac{n}{3}+p-1})\}_{tt}$ ; dark blue in Fig. 21,
- $\{(a_p, b_j), i = 1, \dots, 2p - 1\}_{tt}$ ; dark green in Fig. 21,
- $\{(a_{p+1}, b_j), j = 1, \dots, p - 1\}_{tt}$ ; green in Fig. 21,
- $\{(a_i, b_{2p}), i = 1, \dots, p\}_{ht}$ ; dark red in Fig. 21,
- $\{(a_p, b_j), j = \frac{2n}{3} + 1, \dots, n - 1 - p\}_{ht}$ ; red in Fig. 21,
- $\{(a_{p+1}, b_j), j = n - 1 - p, \dots, n + 1 - p\}_{ht}$ ; pink in Fig. 21,
- $\{(a_i, b_{n+2-p}), i = p + 1, \dots, \frac{n}{3}\}_{ht}$ ; light pink in Fig. 21,
- $\{(a_{n+2-2p}, b_j), j = n + 2 - p, \dots, n\}_{hh}$ ; light gray in Fig. 21,
- $\{(a_i, b_{n+2-p}), i = n + 3 - 2p, \dots, n\}_{hh}$ ; gray in Fig. 21,
- $\{(a_{n+1-2p}, b_j), j = n + 2 - p, \dots, n\}_{ht}$ ; black in Fig. 21.

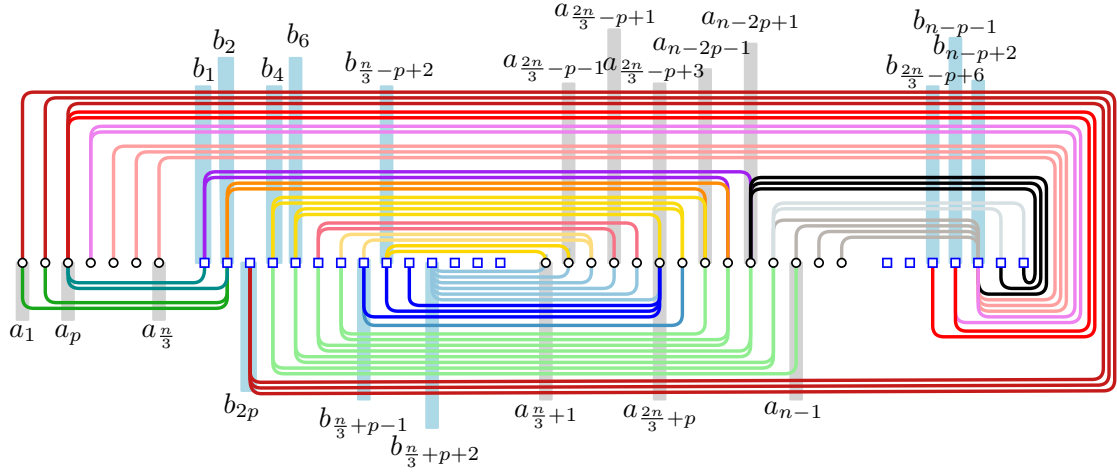


Figure 21: Page  $p = \frac{n}{3} - 7, \dots, \frac{n}{3} - 4$  of  $\mathcal{L}$ .

Page  $\frac{n}{3} - 3$  of  $\mathcal{L}$  contains the following  $\frac{10n}{3} + 11$  edges:

- $\{(a_i, b_{\frac{2n}{3}-6}), i = 1, \dots, \frac{n}{3} - 3\}_{ht}$ ; dark red in Fig. 22,
- $\{(a_{\frac{n}{3}-3}, b_j), j = \frac{2n}{3} + 1, \frac{2n}{3} + 2\}_{ht}$ ; red in Fig. 22,
- $\{(a_{\frac{n}{3}-2}, b_j), j = \frac{2n}{3} + 2, \dots, \frac{2n}{3} + 4\}_{ht}$ ; light red in Fig. 22,
- $\{(a_i, b_{\frac{2n}{3}+4}), i = \frac{n}{3} - 1, \frac{n}{3}\}_{ht}$ ; orange in Fig. 22,
- $\{(a_i, b_1), i = \frac{n}{3} + 6, \frac{n}{3} + 7\}_{hh}$ ; dark orange in Fig. 22,
- $\{(a_i, b_2), i = \frac{n}{3} + 3, \dots, \frac{n}{3} + 6\}_{hh}$ ; light orange in Fig. 22,
- $\{(a_{\frac{n}{3}+3}, b_4)\}_{hh}$ ; dark green in Fig. 22,
- $\{(a_i, b_5), i = \frac{n}{3} + 1, \dots, \frac{n}{3} + 3\}_{hh}$ ; pink in Fig. 22,
- $\{(a_{\frac{n}{3}+7}, b_j), j = \frac{2n}{3} + 4, \dots, n\}_{ht}$ ; yellow in Fig. 22,
- $\{(a_{\frac{n}{3}+8}, b_j), j = \frac{2n}{3} + 5, \dots, n\}_{hh}$ ; dark blue in Fig. 22,
- $\{(a_i, b_{\frac{2n}{3}+6}), i = \frac{n}{3} + 8, \dots, n\}_{hh}$ ; blue in Fig. 22,
- $\{(a_i, b_{\frac{2n}{3}-7}), i = 1, \dots, \frac{n}{3}\}_{tt}$ ; green in Fig. 22,
- $\{(a_{\frac{n}{3}}, b_j), j = 1, \dots, \frac{2n}{3} - 6\}_{tt}$ ; dark pink in Fig. 22,
- $\{(a_{n-1}, b_j), j = \frac{2n}{3} - 5, \frac{2n}{3} - 4\}_{tt}$ ; black in Fig. 22,
- $\{(a_i, b_{\frac{2n}{3}-4}), i = n - 2, n - 3\}_{tt}$ ; gray in Fig. 22,
- $\{(a_{n-3}, b_j), j = \frac{2n}{3} - 3, \frac{2n}{3} - 2\}_{tt}$ ; light blue in Fig. 22,
- $\{(a_i, b_{\frac{2n}{3}-1}), i = \frac{n}{3} + 1, \dots, n - 3\}_{tt}$ ; dark gray in Fig. 22.

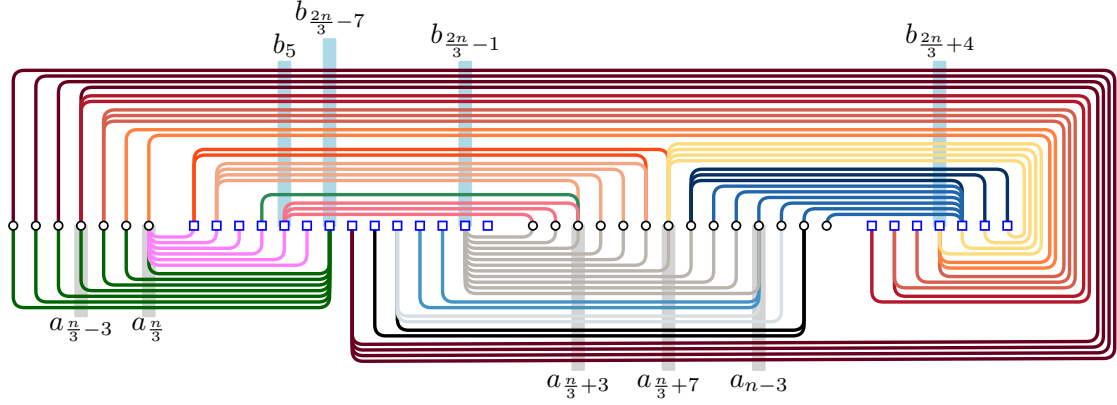


Figure 22: Page  $\frac{n}{3} - 3$  of  $\mathcal{L}$ .

Page  $\frac{n}{3} - 2$  of  $\mathcal{L}$  contains the following  $\frac{10n}{3} + 13$  edges:

- $\{(a_i, b_{\frac{2n}{3}-4}), i = 1, \dots, \frac{n}{3} - 2\}_{ht}$ ; dark red in Fig. 23,
- $\{(a_{\frac{n}{3}-2}, b_{\frac{2n}{3}+1})\}_{ht}$ ; red in Fig. 23,
- $\{(a_{\frac{n}{3}-1}, b_j), j = \frac{2n}{3} + 1, \dots, \frac{2n}{3} + 3\}_{ht}$ ; light red in Fig. 23,
- $\{(a_{\frac{n}{3}}, b_{\frac{2n}{3}+3})\}_{ht}$ ; dark gray in Fig. 23,
- $\{(a_i, b_1), i = \frac{n}{3} + 2, \dots, \frac{n}{3} + 5\}_{hh}$ ; light pink in Fig. 23,
- $\{(a_{\frac{n}{3}+2}, b_2), (a_{\frac{n}{3}+2}, b_4), (a_{\frac{n}{3}+1}, b_4)\}_{hh}$ ; gold in Fig. 23,
- $\{(a_{\frac{n}{3}+5}, b_j), j = \frac{2n}{3} + 3, \dots, n\}_{ht}$ ; gray in Fig. 23
- $\{(a_{\frac{n}{3}+6}, b_j), j = \frac{2n}{3} + 3, \dots, n\}_{hh}$ ; light blue in Fig. 23,
- $\{(a_i, b_{\frac{2n}{3}+3}), i = \frac{2n}{3} + 6, \dots, n\}_{hh}$ ; blue in Fig. 23,
- $\{(a_i, b_{\frac{2n}{3}-5}), i = 1, \dots, \frac{n}{3} - 2\}_{tt}$ ; orange in Fig. 23,
- $\{(a_{\frac{n}{3}-2}, b_j), j = 1, \dots, \frac{2n}{3} - 4\}_{tt}$ ; dark pink in Fig. 23,
- $\{(a_{n-1}, b_{\frac{2n}{3}-3})\}_{tt}$ ; black in Fig. 23,
- $\{(a_{n-2}, b_j), j = \frac{2n}{3} - 3, \dots, \frac{2n}{3}\}_{tt}$ ; pink in Fig. 23,
- $\{(a_i, b_{\frac{2n}{3}}), i = \frac{n}{3} + 1, \dots, n - 3\}_{tt}$ ; dark blue in Fig. 23.

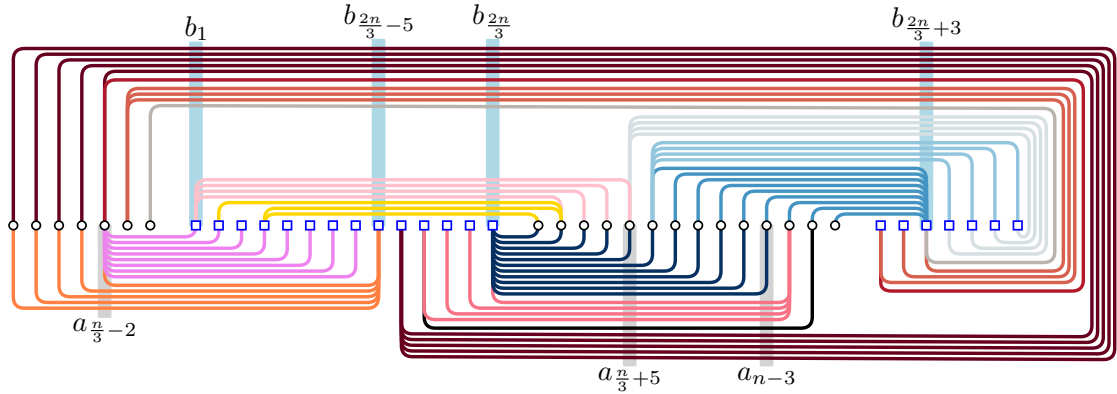


Figure 23: Page  $\frac{n}{3} - 2$  of  $\mathcal{L}$ .

Page  $\frac{n}{3} - 1$  of  $\mathcal{L}$  contains the following  $\frac{11n}{3} - 8$  edges:

- $\{(a_i, b_{\frac{2n}{3}-3}), i = 1, \dots, \frac{n}{3} - 1\}_{hh}$ ; dark red in Fig. 24,
- $\{(a_{\frac{n}{3}-1}, b_j), j = 1, \dots, \frac{2n}{3} - 4\}_{hh}$ ; light red in Fig. 24,
- $\{(a_i, b_{\frac{2n}{3}-2}), i = 1, \dots, \frac{n}{3} - 1\}_{th}$ ; red in Fig. 24,
- $\{(a_{n-1}, b_j), j = \frac{2n}{3} - 2, \dots, \frac{2n}{3}\}_{ht}$ ; light orange in Fig. 24,
- $\{(a_{\frac{n}{3}+2}, b_{\frac{2n}{3}+1})\}_{ht}$ ; dark blue in Fig. 24,
- $\{(a_{\frac{n}{3}+3}, b_j), j = \frac{2n}{3} + 1, \dots, n\}_{ht}$ ; gray in Fig. 24,
- $\{(a_{\frac{n}{3}+4}, b_j), j = \frac{2n}{3} + 3, \dots, n\}_{hh}$ ; light blue in Fig. 24,
- $\{(a_{\frac{n}{3}+5}, b_{\frac{2n}{3}+2}), (a_{\frac{n}{3}+5}, b_{\frac{2n}{3}+3})\}_{hh}$ ; green in Fig. 24,
- $\{(a_i, b_{\frac{2n}{3}+2}), i = \frac{n}{3} + 6, \dots, n\}_{hh}$ ; blue in Fig. 24,
- $\{(a_{n-1}, b_1), (a_{n-2}, b_1), (a_{n-2}, b_2), (a_{n-3}, b_2)\}_{tt}$ ; orange in Fig. 24,
- $\{(a_i, b_j), (a_{i-1}, b_j), i = n - 3, \dots, \frac{2n}{3} + 2, j = 4, \dots, \frac{n}{3} - 2\}_{tt}$ ; yellow in Fig. 24,
- $\{(a_i, b_{\frac{n}{3}-1}), i = \frac{2n}{3} + 2, \dots, \frac{2n}{3}\}_{tt}$ ; pink in Fig. 24,
- $\{(a_{\frac{2n}{3}}, b_j), j = \frac{n}{3}, \frac{n}{3} + 1\}_{tt}$ ; black in Fig. 24,
- $\{(a_i, b_{\frac{n}{3}+2}), i = \frac{n}{3} + 1, \dots, \frac{2n}{3}\}_{tt}$ ; dark pink in Fig. 24,

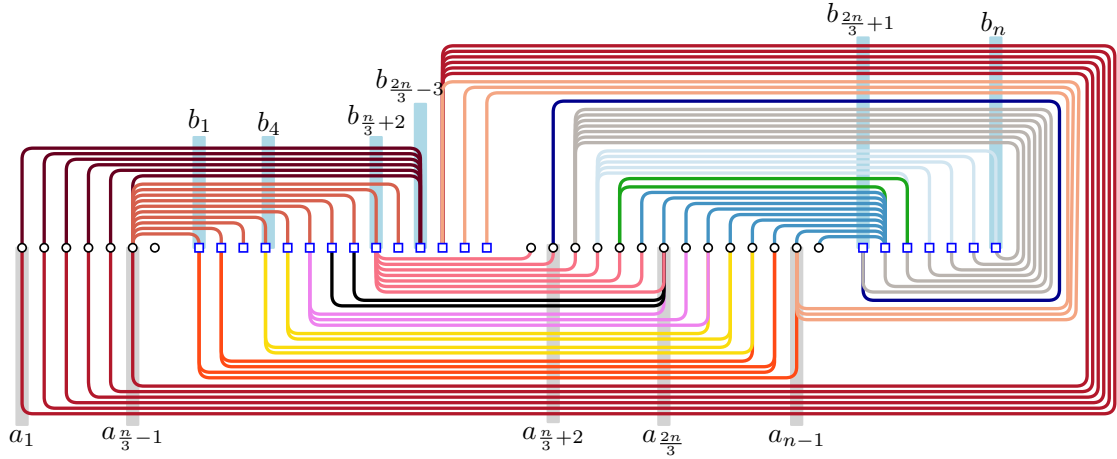


Figure 24: Page  $\frac{n}{3} - 1$  of  $\mathcal{L}$ .

Page  $\frac{n}{3}$  of  $\mathcal{L}$  contains the following  $4n + 14$  edges:

- $\{(a_i, b_{\frac{2n}{3}}), i = 1, \dots, \frac{n}{3}\}_{ht}$ ; dark red in Fig. 25,
- $\{(a_{\frac{n}{3}+1}, b_j), j = 1, 2, 3\}_{ht}$ ; red in Fig. 25,
- $\{(a_i, b_3), i = \frac{n}{3} + 1, \dots, n\}_{ht}$ ; dark orange in Fig. 25,
- $\{(a_n, b_j), j = 4, \dots, \frac{2n}{3}\}_{ht}$ ; orange in Fig. 25,
- $\{(a_{\frac{n}{3}+2}, b_j), j = \frac{2n}{3} + 2, \dots, n\}_{hh}$ ; gray in Fig. 25,
- $\{(a_{\frac{n}{3}+4}, b_{\frac{2n}{3}+2})\}_{hh}$ ; yellow in Fig. 25,
- $\{(a_i, b_{\frac{2n}{3}+1}), i = \frac{n}{3} + 4, \dots, n\}_{hh}$ ; light blue in Fig. 25,
- $\{(a_{\frac{n}{3}+1}, b_j), j = \frac{2n}{3} + 1, \dots, n\}_{ht}$ ; light orange in Fig. 25,
- $\{(a_i, b_{\frac{2n}{3}-1}), i = 1, \dots, \frac{n}{3}\}_{ht}$ ; dark blue in Fig. 25,
- $\{(a_{\frac{n}{3}}, b_j), j = 1, \dots, \frac{2n}{3} - 1\}_{ht}$ ; blue in Fig. 25.

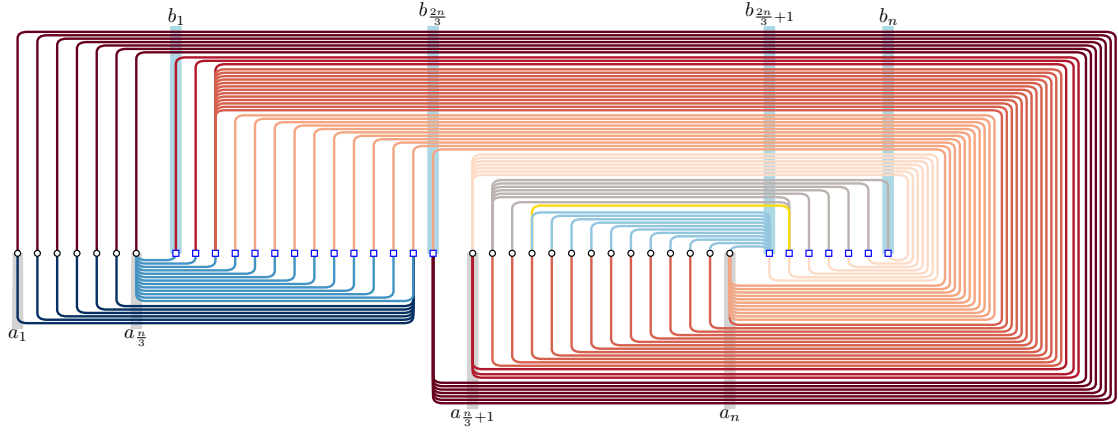


Figure 25: Page  $\frac{n}{3}$  of  $\mathcal{L}$ .

So, in total  $\mathcal{L}$  has  $2n + 16 + \frac{8n}{3} + 5 + \sum_{p=3}^4 (\frac{8n}{3} + p + 5) + \sum_{p=\frac{n}{3}-7}^{\frac{n}{3}-4} (\frac{8n}{3} - 2p - 1) + \sum_{p=5}^{\frac{n}{3}-8} (\frac{8n}{3} + 2p + 18) + \frac{10n}{3} + 11 + \frac{10n}{3} + 13 + \frac{11n}{3} - 8 + 4n + 14 = n^2$  edges. Since no two edges have been assigned to the same deque and all edges in the same deque form a cylindric layout, it follows that the deque number of  $K_{n,n}$  is at most  $\frac{n}{3}$ .  $\square$

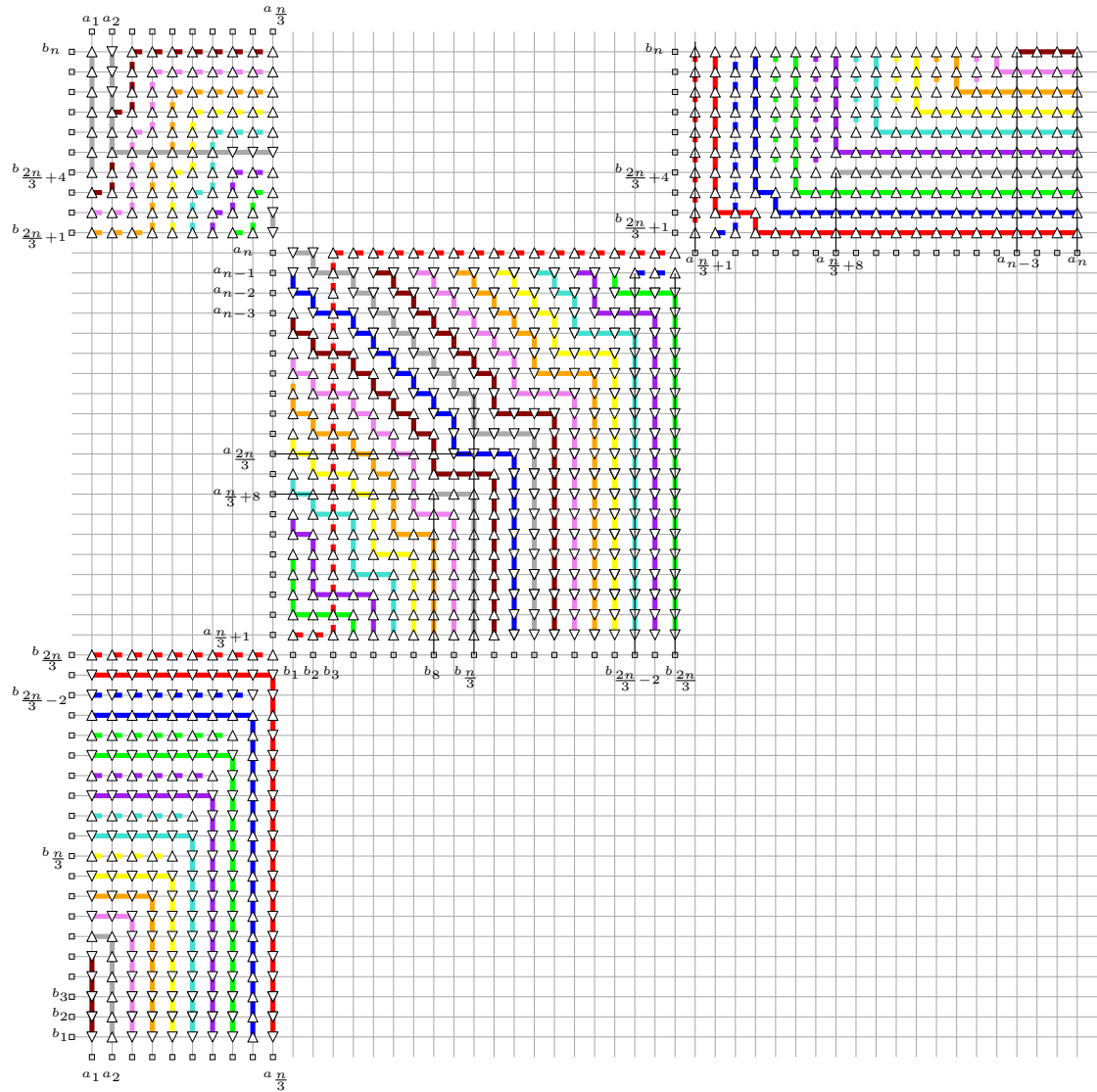


Figure 26: Illustration of the grid representation of a deque layout of  $K_{n,n}$ , in which paths of the same color correspond to the same deque. The points of the grid that are represented by a triangle pointing up (down) correspond to head- $\star$  (tail- $\star$ , resp.) edges; grid points covered by a solid line are head-head or tail-tail edges; the dashed covered ones are head-tail or tail-head

We complete this section by providing our upper bound on the rique-number of  $K_{n,n}$ .

**Theorem 7.** *The rique-number of the complete bipartite graph  $K_{n,n}$  is at most  $\lfloor \frac{n-1}{2} \rfloor - 1$ .*

*Proof.* For the proof, we distinguish two cases depending on whether  $n$  is odd or even.

**Case 1:**  $n$  is odd. We first assume that  $n$  is odd and we prove that  $K_{n,n}$  admits a rique layout  $\mathcal{L}$  with  $\lfloor \frac{n}{2} \rfloor - 1$  riques. Let  $A = \{a_1, \dots, a_n\}$  and  $B = \{b_1, \dots, b_n\}$  be the two parts of  $K_{n,n}$ , such that  $a_1 \prec b_1 \prec a_2 \prec b_2 \prec \dots \prec a_{\lfloor \frac{n}{2} \rfloor} \prec b_{\lfloor \frac{n}{2} \rfloor} \prec b_{\lceil \frac{n}{2} \rceil} \prec \dots \prec b_n \prec a_{\lceil \frac{n}{2} \rceil} \prec \dots \prec a_n$  holds in  $\mathcal{L}$ . In  $\mathcal{L}$ , there exist 12 special riques, in particular, the ones in  $\{1, 2, 3, 4, 5, 6, 7, \lfloor \frac{n}{2} \rfloor - 5, \lfloor \frac{n}{2} \rfloor - 4, \lfloor \frac{n}{2} \rfloor - 3, \lfloor \frac{n}{2} \rfloor - 2, \lfloor \frac{n}{2} \rfloor - 1\}$ ; see Fig. 45.

Page 1 of  $\mathcal{L}$  contains the following  $3n$  edges:

- $\{(a_1, b_j), j = 1, \dots, n\}_{ht}$ ; dark red in Fig. 27,
- $\{(a_i, b_1), i = \lceil \frac{n}{2} \rceil, \dots, n\}_{ht}$ ; red in Fig. 27,
- $\{(a_{\lfloor \frac{n}{2} \rfloor}, b_j), j = 2, \dots, \lfloor \frac{n}{2} \rfloor\}_{hh}$ ; gray in Fig. 27,
- $\{(a_i, b_2), i = \lceil \frac{n}{2} \rceil, \dots, n\}_{hh}$ ; blue in Fig. 27,
- $\{(a_{\lceil \frac{n}{2} \rceil}, b_j), j = \lceil \frac{n}{2} \rceil, \dots, n\}_{hh}$ ; light blue in Fig. 27.

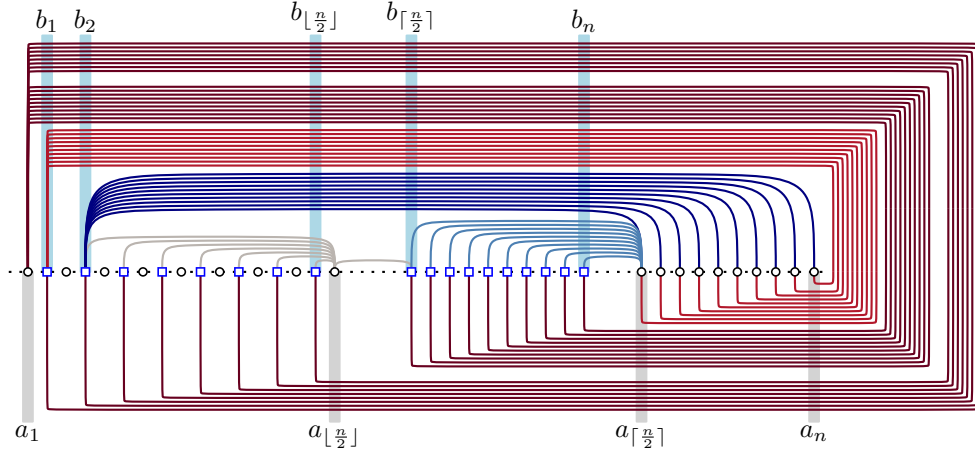


Figure 27: Page 1 of  $\mathcal{L}$  when  $n$  is odd.

Page 2 of  $\mathcal{L}$  contains the following  $\frac{5n-1}{2} + 1$  edges:

- $\{(a_i, b_1), i = 2, \dots, \lfloor \frac{n}{2} \rfloor\}_{ht}$ ; dark red in Fig. 28,
- $\{(a_2, b_{\lfloor \frac{n}{2} \rfloor})\}_{ht}$ ; yellow in Fig. 28,
- $\{(a_2, b_j), j = \lceil \frac{n}{2} \rceil, \dots, n\}_{ht}$ ; light red in Fig. 28,
- $\{(a_3, b_n)\}_{ht}$ ; red in Fig. 28,
- $\{(a_i, b_3), i = \lceil \frac{n}{2} \rceil, \dots, n\}_{ht}$ ; dark blue in Fig. 28,
- $\{(a_{n-3}, b_j), j = \lfloor \frac{n}{2} \rfloor - 2, \dots, \lceil \frac{n}{2} \rceil + 1\}_{hh}$ ; light blue in Fig. 28,
- $\{(a_i, b_{\lceil \frac{n}{2} \rceil + 1}), i = \lceil \frac{n}{2} \rceil + 1, \dots, n-4\}_{hh}$ ; blue in Fig. 28,
- $\{(a_{\lceil \frac{n}{2} \rceil + 1}, b_j), j = \lceil \frac{n}{2} \rceil + 2, \dots, n\}_{hh}$ ; gray in Fig. 28.



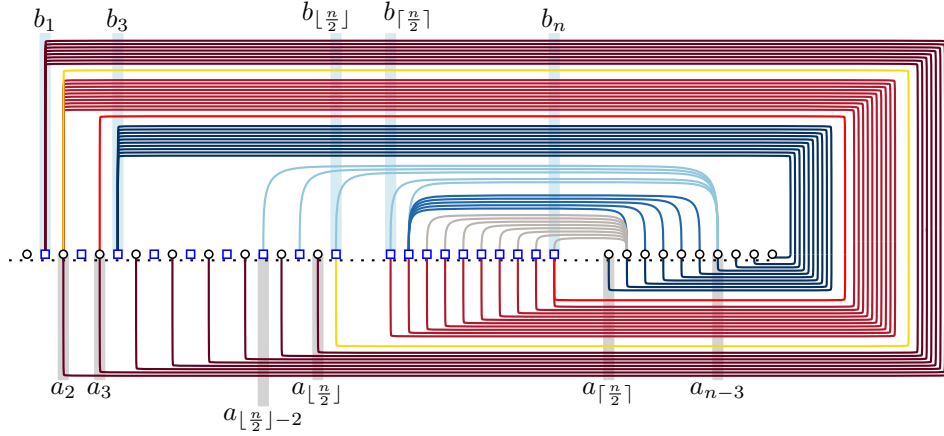


Figure 28: Page 2 of  $\mathcal{L}$  when  $n$  is odd.

For  $p = 3, 4, 5$ , page  $p$  of  $\mathcal{L}$  contains the following  $\left(\frac{5n-1}{2}\right) + 1$  edges

- $\{(a_{p-1}, b_j), j = 2, \dots, \lfloor \frac{n}{2} \rfloor - p + 2\}_{ht}$ ; dark red in Fig. 29,
- $\{(a_p, b_j), j = \lfloor \frac{n}{2} \rfloor - p + 2, \dots, n - p + 2\}_{ht}$ ; red in Fig. 29,
- $\{(a_{p+1}, b_j), j = n - p + 2, \dots, n\}_{ht}$ ; light red in Fig. 29,
- $\{(a_i, b_{p+1}), i = \lceil \frac{n}{2} \rceil, \dots, n\}_{ht}$ ; dark blue in Fig. 29,
- $\{(a_{n+(p-5)}, b_j), j = \lfloor \frac{n}{2} \rfloor - 2, \dots, \lfloor \frac{n}{2} \rfloor + (p-1)\}_{hh}$ ; gray in Fig. 29,
- $\{(a_i, b_{\lfloor \frac{n}{2} \rfloor + (p-1)}), i = \lceil \frac{n}{2} \rceil + (p-1), \dots, n + (p-6)\}_{hh}$ ; blue in Fig. 29,
- $\{(a_{\lceil \frac{n}{2} \rceil + (p-1)}, b_j), j = \lceil \frac{n}{2} \rceil + p, \dots, n\}_{hh}$ ; light blue in Fig. 29.

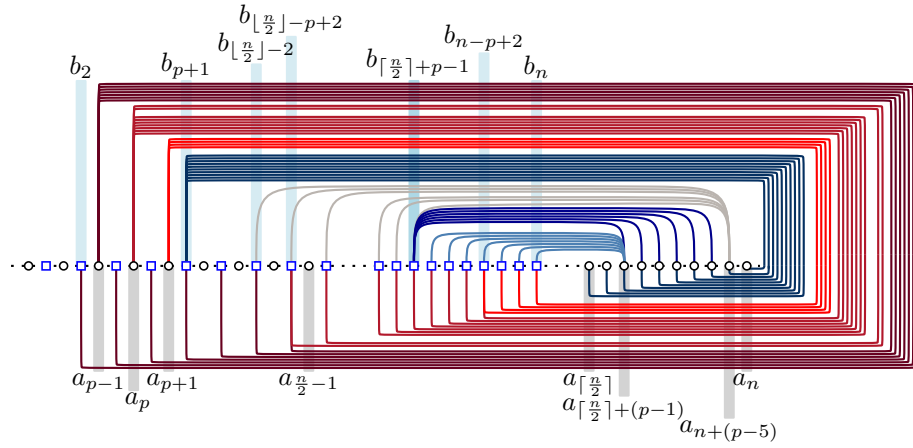


Figure 29: Page  $p = 3, 4, 5$  of  $\mathcal{L}$  when  $n$  is odd.

Page 6 of  $\mathcal{L}$  contains the following  $\frac{5n-1}{2} - 8$  edges:

- $\{(a_5, b_j), j = 2, \dots, \lfloor \frac{n}{2} \rfloor - 4\}_{ht}$ ; dark red in Fig. 30,
- $\{(a_6, b_j), j = \lfloor \frac{n}{2} \rfloor - 4, \dots, n - 4\}_{ht}$ ; red in Fig. 30,
- $\{(a_7, b_j), j = n - 4, \dots, n\}_{ht}$ ; light red in Fig. 30,
- $\{(a_i, b_7), i = \lceil \frac{n}{2} \rceil, \dots, n\}_{ht}$ ; dark blue in Fig. 30,
- $\{(a_i, b_{\lceil \frac{n}{2} \rceil + 5}), i = \lceil \frac{n}{2} \rceil + 5, \dots, n\}_{hh}$ ; blue in Fig. 30,
- $\{(a_{\lceil \frac{n}{2} \rceil + 5}, b_j), j = \lceil \frac{n}{2} \rceil + 6, \dots, n\}_{hh}$ ; light red in Fig. 30.

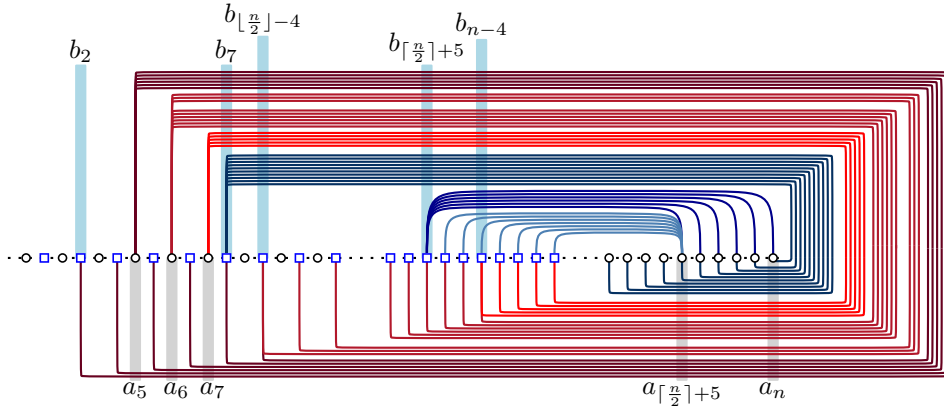


Figure 30: Page 6 of  $\mathcal{L}$  when  $n$  is odd.

Page 7 of  $\mathcal{L}$  contains the following  $\frac{3n+1}{2} + 4$  edges:

- $\{(a_6, b_j), j = 2, \dots, \lfloor \frac{n}{2} \rfloor - 5\}_{ht}$ ; dark red in Fig. 31,
- $\{(a_7, b_j), j = \lfloor \frac{n}{2} \rfloor - 5, \dots, n - 5\}_{ht}$ ; red in Fig. 31,
- $\{(a_8, b_j), j = n - 5, \dots, n\}_{ht}$ ; light red in Fig. 31,

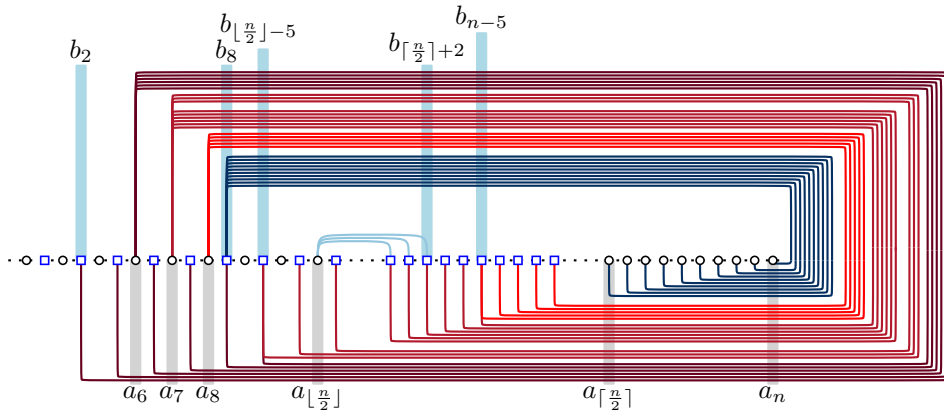


Figure 31: Page 7 of  $\mathcal{L}$  when  $n$  is odd.

- $\{(a_i, b_8), i = \lceil \frac{n}{2} \rceil, \dots, n\}_{ht}$ ; blue in Fig. 31,
- $\{(a_{\lfloor \frac{n}{2} \rfloor}, b_j), j = \lceil \frac{n}{2} \rceil, \dots, \lceil \frac{n}{2} \rceil + 2\}_{hh}$ ; light blue in Fig. 31.

For  $p = 8, \dots, \frac{n-1}{2} - 6$ , page  $p$  of  $\mathcal{L}$  contains the following  $\frac{5n+3}{2} - 2p + 4$  edges:

- $\{(a_{p-1}, b_j), j = 2, \dots, \lfloor \frac{n}{2} \rfloor - p + 2\}_{ht}$ ; dark red in Fig. 32,
- $\{(a_p, b_j), j = \lfloor \frac{n}{2} \rfloor - p + 2, \dots, n - p + 2\}_{ht}$ ; red in Fig. 32,
- $\{(a_{p+1}, b_j), j = n - p + 2, \dots, n\}_{ht}$ ; light red in Fig. 32,
- $\{(a_i, b_{p+1}), i = \lceil \frac{n}{2} \rceil, \dots, n\}_{ht}$ ; dark blue in Fig. 32,
- $\{(a_i, b_{\lceil \frac{n}{2} \rceil + p - 2}), i = \lceil \frac{n}{2} \rceil + p - 2, \dots, n\}_{hh}$ ; blue in Fig. 32,
- $\{(a_{\lceil \frac{n}{2} \rceil + p - 2}, b_j), j = \lceil \frac{n}{2} \rceil + p - 1, \dots, n\}_{hh}$ ; light blue in Fig. 32.

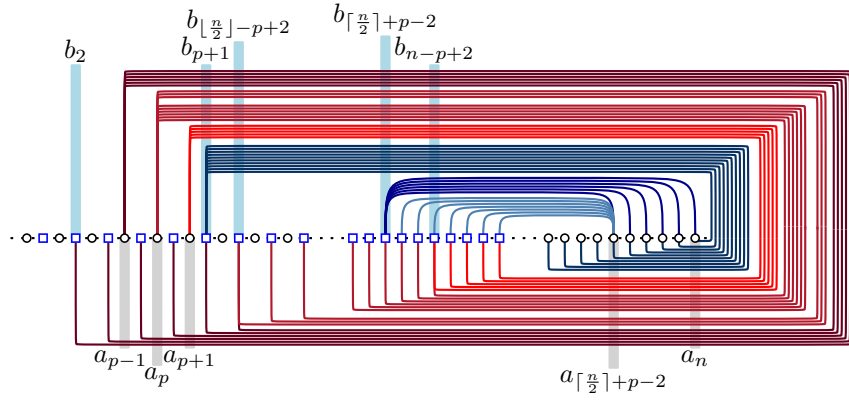


Figure 32: Page  $p = 8, \dots, \frac{n-1}{2} - 6$  of  $\mathcal{L}$  when  $n$  is odd.

Page  $\frac{n-1}{2} - 5$  of  $\mathcal{L}$  contains the following  $2n-3$  edges:

- $\{(a_{\lfloor \frac{n}{2} \rfloor - 6}, b_j), j = 2, \dots, \lfloor \frac{n}{2} \rfloor - 7\}_{ht}$ ; dark red in Fig. 33,
- $\{(a_{\lfloor \frac{n}{2} \rfloor - 5}, b_j), j = \lfloor \frac{n}{2} \rfloor - 7, \dots, n - 7\}_{ht}$ ; red in Fig. 33,
- $\{(a_{\lfloor \frac{n}{2} \rfloor - 4}, b_j), j = n - 7, \dots, n\}_{ht}$ ; light red in Fig. 33,
- $\{(a_i, b_{\lfloor \frac{n}{2} \rfloor - 4}), i = \lceil \frac{n}{2} \rceil, \dots, n\}_{ht}$ ; light blue in Fig. 33,
- $\{(a_i, b_{\lfloor \frac{n}{2} \rfloor - 3}), i = \lceil \frac{n}{2} \rceil + 5, \dots, n\}_{hh}$ ; blue in Fig. 33.

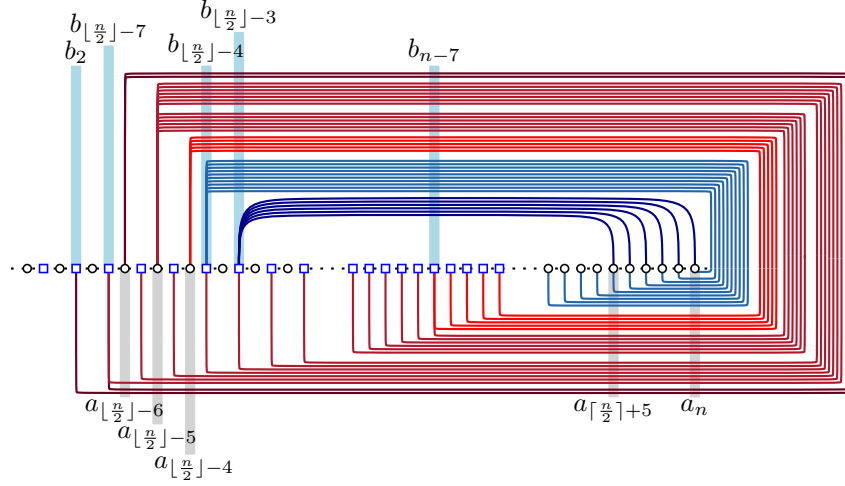


Figure 33: Page  $\frac{n-1}{2} - 5$  of  $\mathcal{L}$  when  $n$  is odd.

For  $p = \frac{n-1}{2} - k$ , with  $k \in \{4, 3, 2\}$ , page  $p$  of  $\mathcal{L}$  contains the following  $\frac{3n-1}{2} - 2k + 20$  edges:

- $\{(a_{p-1}, b_j), j = 2, \dots, \lfloor \frac{n}{2} \rfloor - p - 4\}_{ht}$ ; dark red in Fig. 34,
- $\{(a_p, b_j), j = \lfloor \frac{n}{2} \rfloor - p - 4, \dots, n - p - 4\}_{ht}$ ; red in Fig. 34,
- $\{(a_{p+1}, b_j), j = n - p - 4, \dots, n\}_{ht}$ ; light red in Fig. 34,
- $\{(a_i, b_{p+1}), i = \lceil \frac{n}{2} \rceil, \dots, \lceil \frac{n}{2} \rceil + k\}_{ht}$ ; dark pink in Fig. 34,
- $\{(a_i, b_{p+2}), i = \lceil \frac{n}{2} \rceil + k, \dots, n - 8 + k\}_{ht}$ ; light pink in Fig. 34,
- $\{(a_{n-8+k}, b_j), j = \lfloor \frac{n}{2} \rfloor - 2 + k, \dots, \lceil \frac{n}{2} \rceil\}_{ht}$ ; pink in Fig. 34,
- $\{(a_i, b_{n+(2k-9)}), i = n + (k - 8), \dots, n\}_{ht}$ ; dark blue in Fig. 34,
- $\{(a_i, b_{n+(2k-8)}), i = n + (k - 8), \dots, n\}_{hh}$ ; blue in Fig. 34,
- $\{(a_{n+(k-8)}, b_j), j = n + (2k - 7), \dots, n\}_{hh}$ ; gray in Fig. 34.

Page  $\frac{n-1}{2} - 1$  of  $\mathcal{L}$  contains the following  $\frac{3n+1}{2} + 18$  edges:

- $\{(a_{\lfloor \frac{n}{2} \rfloor - 1}, b_j), j = 2, \dots, \lceil \frac{n}{2} \rceil + 3\}_{ht}$ ; dark red in Fig. 35,
- $\{(a_{\lfloor \frac{n}{2} \rfloor}, b_j), j = \lceil \frac{n}{2} \rceil + 3, \dots, n\}_{ht}$ ; red in Fig. 35,
- $\{(a_i, b_{\lfloor \frac{n}{2} \rfloor}), i = \lceil \frac{n}{2} \rceil, \lceil \frac{n}{2} \rceil + 1\}_{ht}$ ; light red in Fig. 35,
- $\{(a_i, b_{\lceil \frac{n}{2} \rceil}), i = \lceil \frac{n}{2} \rceil + 1, \dots, n - 7\}_{ht}$ ; dark pink in Fig. 35,

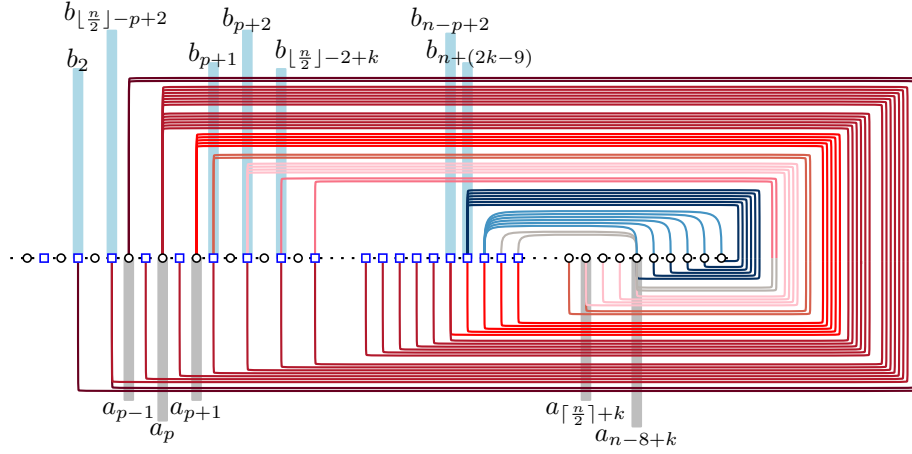


Figure 34: Page  $p = \frac{n-1}{2} - k$ , with  $k \in \{4, 3, 2\}$  of  $\mathcal{L}$  when  $n$  is odd.

- $\{(a_i, b_{n-7}), i = \lceil \frac{n}{4} \rceil + 1, \dots, n\}_{ht}$ ; pink in Fig. 35,
- $\{(a_i, b_{n-6}), i = \lfloor \frac{n}{4} \rfloor + 1, \dots, n\}_{hh}$ ; dark blue in Fig. 35,
- $\{(a_{\lceil \frac{n}{4} \rceil + 1}, b_j), j = n - 5, \dots, n\}_{hh}$ ; blue in Fig. 35,
- $\{(a_{\lfloor \frac{n}{2} \rfloor - 2}, b_j), j = 2, 3\}_{hh}$ ; gray in Fig. 35.

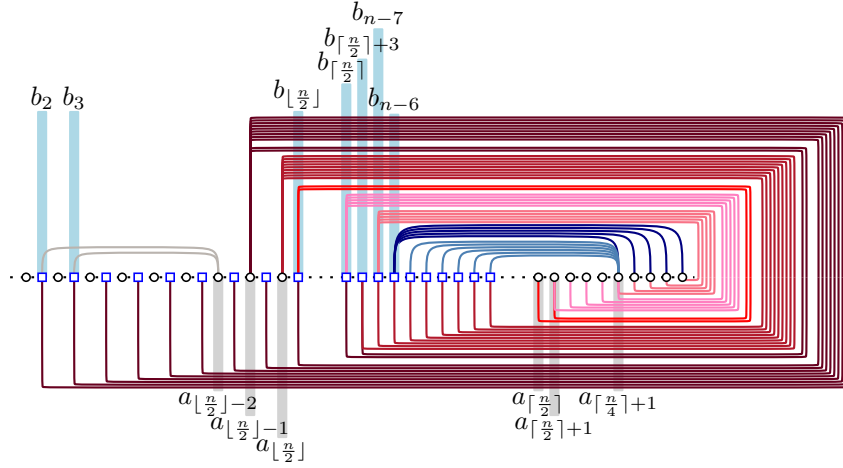


Figure 35: Page  $\frac{n-1}{2} - 1$  of  $\mathcal{L}$  when  $n$  is odd.

So, in total  $\mathcal{L}$  has  $3n + \frac{5n-1}{2} + 1 + 3 \left( \frac{5n-1}{2} + 1 \right) + \frac{5n-1}{2} - 8 + \frac{3n+1}{2} + 4 + \sum_{p=8}^{\frac{n-1}{2}-6} \left( \frac{5n+3}{2} - 2p + 4 \right) + 2n - 3 + \sum_{k=2}^4 \left( \frac{3n-1}{2} - 2k + 20 \right) + \left( \frac{3n+1}{2} + 18 \right) = n^2$  edges. Since no two edges in the same rique deviate from the properties of cylindric layouts, it follows that the rique number of  $k_{n,n}$  is at most  $\lfloor \frac{n-1}{2} \rfloor - 1$  when  $n$  is odd.

**Case 2:**  $n$  is even. When  $n$  is even, we prove that  $K_{n,n}$  admits a rique layout  $\mathcal{L}$  with  $\frac{n}{2} - 2$  riques. Let  $A = \{a_1, \dots, a_n\}$  and  $B = \{b_1, \dots, b_n\}$  be the two parts of  $K_{n,n}$ , such that  $a_1 < b_1 <$

$a_2 \prec b_2 \prec \dots \prec a_{\frac{n}{2}-1} \prec b_{\frac{n}{2}-1} \prec b_{\frac{n}{2}} \prec \dots \prec b_n \prec a_{\frac{n}{2}} \prec \dots \prec a_n$  holds in  $\mathcal{L}$ . In  $\mathcal{L}$ , there exist 12 special riques, in particular, the ones in  $\{1, 2, 3, 4, 5, 6, 7, \frac{n}{2} - 6, \frac{n}{2} - 5, \frac{n}{2} - 4, \frac{n}{2} - 3, \frac{n}{2} - 2\}$ ; see Fig. 46.

Page 1 of  $\mathcal{L}$  contains the following  $3n + 1$  edges:

- $\{(a_1, b_j), j = 1, \dots, n\}_{ht}$ ; dark red in Fig. 36,
- $\{(a_i, b_1), i = \frac{n}{2}, \dots, n\}_{ht}$ ; red in Fig. 36,
- $\{(a_{\frac{n}{2}-1}, b_j), j = 2, \dots, \frac{n}{2} - 1\}_{hh}$ ; light blue in Fig. 36,
- $\{(a_i, b_2), i = \frac{n}{2}, \dots, n\}_{hh}$ ; light red in Fig. 36,
- $\{(a_{\frac{n}{2}}, b_j), j = \frac{n}{2}, \dots, n\}_{hh}$ ; blue in Fig. 36.

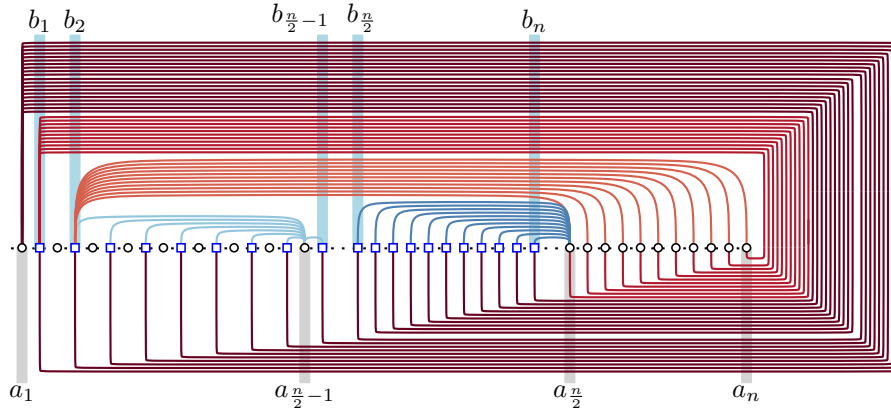


Figure 36: Page 1 of  $\mathcal{L}$  when  $n$  is even.

Page 2 of  $\mathcal{L}$  contains the following  $\frac{5n}{2} + 2$  edges:

- $\{(a_i, b_1), i = 2, \dots, \frac{n}{2} - 1\}_{ht}$ ; dark red in Fig. 37,
- $\{(a_2, b_{\frac{n}{2}-1})\}_{ht}$ ; orange in Fig. 37,

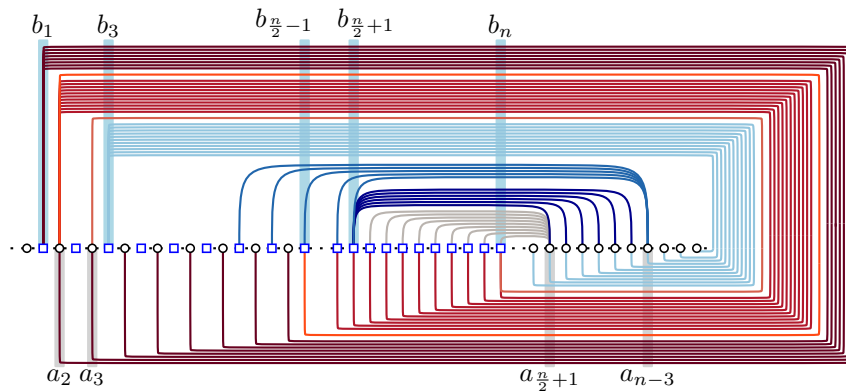


Figure 37: Page 2 of  $\mathcal{L}$  when  $n$  is even.

- $\{(a_2, b_j), j = \frac{n}{2}, \dots, n\}_{ht}$ ; red in Fig. 37,
- $\{(a_3, b_n)\}_{ht}$ ; light red in Fig. 37,
- $\{(a_i, b_3), i = \frac{n}{2}, \dots, n\}_{ht}$ ; light blue in Fig. 37,
- $\{(a_{n-3}, b_j), j = \frac{n}{2} - 3, \dots, \frac{n}{2} + 1\}_{hh}$ ; blue in Fig. 37,
- $\{(a_i, b_{\frac{n}{2}+1}), i = \frac{n}{2} + 1, \dots, n - 4\}_{hh}$ ; dark blue in Fig. 37,
- $\{(a_{\frac{n}{2}+1}, b_j), j = \frac{n}{2} + 2, \dots, n\}_{hh}$ ; gray in Fig. 37.

For  $p = 3, 4, 5$ , page  $p$  of  $\mathcal{L}$  contains the following  $\frac{5n}{2} + 2$  edges

- $\{(a_{p-1}, b_j), j = 2, \dots, \frac{n}{2} - p + 1\}_{ht}$ ; dark red in Fig. 38,
- $\{(a_p, b_j), j = \frac{n}{2} - p + 1, \dots, n - p + 2\}_{ht}$ ; red in Fig. 38,
- $\{(a_{p+1}, b_j), j = n - p + 2, \dots, n\}_{ht}$ ; light red in Fig. 38,
- $\{(a_i, b_{p+1}), i = \frac{n}{2}, \dots, n\}_{ht}$ ; dark blue in Fig. 38,
- $\{(a_{n+p-6}, b_j), j = \frac{n}{2} - 3, \dots, \frac{n}{2} + p - 1\}_{hh}$ ; light blue in Fig. 38,
- $\{(a_i, b_{\frac{n}{2}+(p-1)}), i = \frac{n}{2} + (p - 1), \dots, n + (p - 6)\}_{hh}$ ; blue in Fig. 38,
- $\{(a_{\frac{n}{2}+(p-1)}, b_j), j = \frac{n}{2} + p, \dots, n\}_{hh}$ ; gray in Fig. 38.

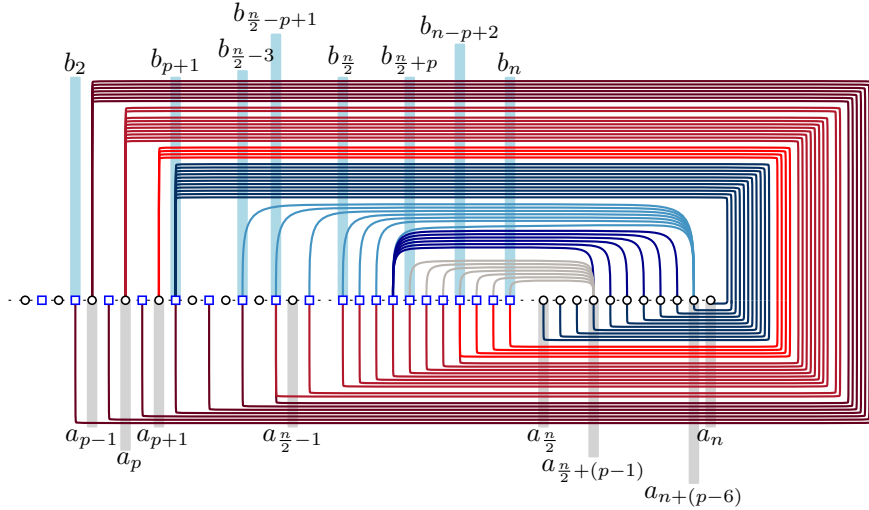


Figure 38: Page  $p = 3, 4, 5$  of  $\mathcal{L}$  when  $n$  is even.

Page 6 of  $\mathcal{L}$  contains the following  $\frac{5n}{2} - 7$  edges:

- $\{(a_5, b_j), j = 2, \dots, \frac{n}{2} - 5\}_{ht}$ ; dark red in Fig. 39,
- $\{(a_6, b_j), j = \frac{n}{2} - 5, \dots, n - 4\}_{ht}$ ; red in Fig. 39,
- $\{(a_7, b_j), j = n - 4, \dots, n\}_{ht}$ ; light red in Fig. 39,
- $\{(a_i, b_7), i = \frac{n}{2}, \dots, n\}_{ht}$ ; dark blue in Fig. 39,
- $\{(a_i, b_{\frac{n}{2}+5}), i = \frac{n}{2} + 5, \dots, n\}_{hh}$ ; blue in Fig. 39,
- $\{(a_{\frac{n}{2}+5}, b_j), j = \frac{n}{2} + 6, \dots, n\}_{hh}$ ; gray in Fig. 39.

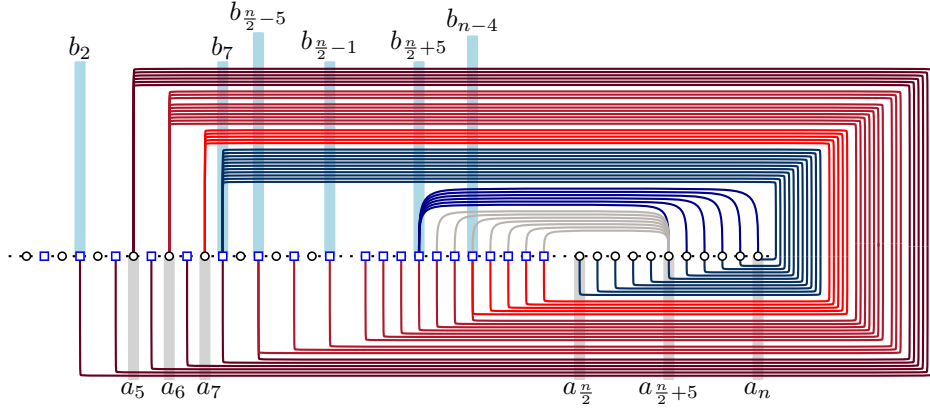


Figure 39: Page 6 of  $\mathcal{L}$  when  $n$  is even.

Page 7 of  $\mathcal{L}$  contains the following  $\frac{3n}{2} + 23$  edges:

- $\{(a_6, b_j), j = 2, \dots, \frac{n}{2} - 6\}_{ht}$ ; dark red in Fig. 40,
- $\{(a_7, b_j), j = \frac{n}{2} - 6, \dots, n - 5\}_{ht}$ ; red in Fig. 40,
- $\{(a_8, b_j), j = n - 5, \dots, n\}_{ht}$ ; light red in Fig. 40,
- $\{(a_i, b_8), i = \frac{n}{2}, \dots, n\}_{ht}$ ; dark blue in Fig. 40,
- $\{(a_{\frac{n}{2}-1}, b_j), j = \frac{n}{2}, \dots, \frac{n}{2} + 3\}_{hh}$ ; gray in Fig. 40,
- $\{(a_{n-8}, b_j), j = n - 8, \dots, n\}_{hh}$ ; blue in Fig. 40,
- $\{(a_i, b_{n-8}), i = n - 7, \dots, n\}_{hh}$ ; light blue in Fig. 40.

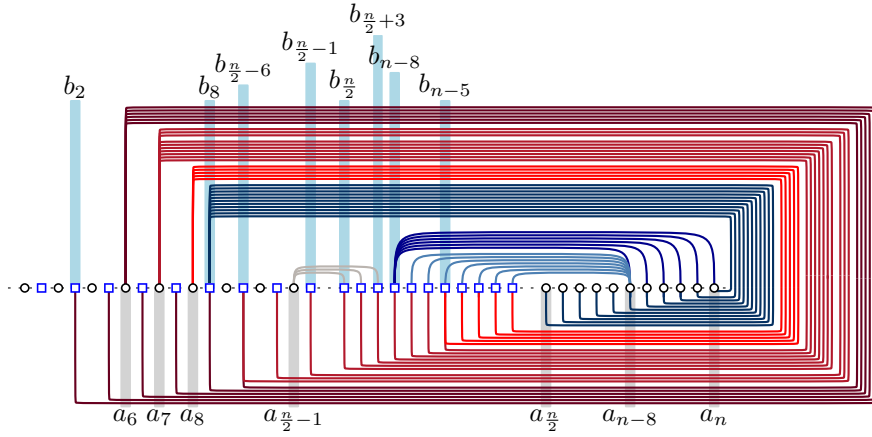


Figure 40: Page 7 of  $\mathcal{L}$  when  $n$  is even.

For  $p = 8, \dots, \frac{n}{2} - 7$ , page  $p$  of  $\mathcal{L}$  contains the following  $\frac{5n}{2} - 2p + 7$  edges:

- $\{(a_{p-1}, b_j), j = 2, \dots, \frac{n}{2} - p + 1\}_{ht}$ ; dark red in Fig. 41,
- $\{(a_p, b_j), j = \frac{n}{2} - p + 1, \dots, n - p + 2\}_{ht}$ ; red in Fig. 41,



- $\{(a_{p+1}, b_j), j = n - p + 2, \dots, n\}_{ht}$ ; light red in Fig. 41,
- $\{(a_i, b_{p+1}), i = \frac{n}{2}, \dots, n\}_{ht}$ ; dark blue in Fig. 41,
- $\{(a_i, b_{\frac{n}{2}+p-2}), i = \frac{n}{2} + (p-2), \dots, n\}_{hh}$ ; blue in Fig. 41,
- $\{(a_{\frac{n}{2}+(p-2)}, b_j), j = \frac{n}{2} + (p-1), \dots, n\}_{hh}$ ; light blue in Fig. 41.

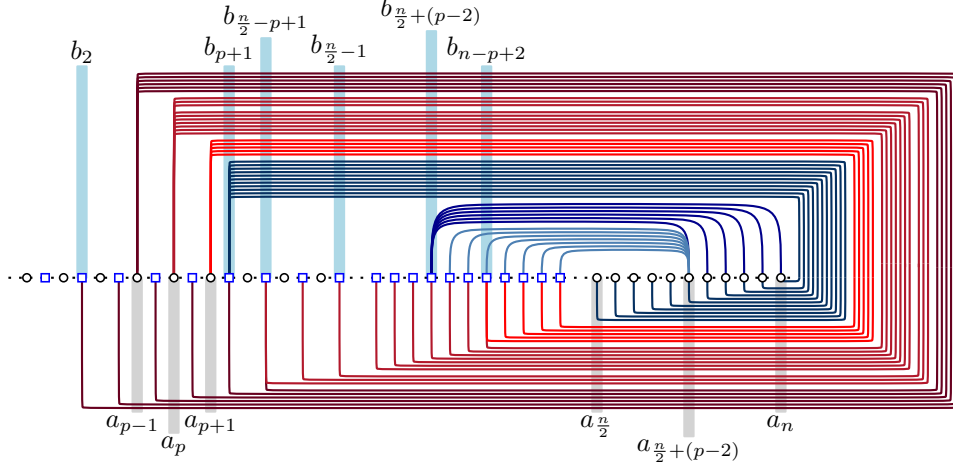


Figure 41: Page  $p = 8, \dots, \frac{n}{2} - 7$  of  $\mathcal{L}$  when  $n$  is even.

Page  $\frac{n}{2} - 6$  of  $\mathcal{L}$  contains the following  $2n-2$  edges:

- $\{(a_{\frac{n}{2}-7}, b_j), j = 2, \dots, \frac{n}{2} - 8\}_{ht}$ ; dark red in Fig. 42,
- $\{(a_{\frac{n}{2}-6}, b_j), j = \frac{n}{2} - 8, \dots, n - 7\}_{ht}$ ; red in Fig. 42,
- $\{(a_{\frac{n}{2}-5}, b_j), j = n - 7, \dots, n\}_{ht}$ ; light red in Fig. 42,
- $\{(a_i, b_{\frac{n}{2}-5}), i = \frac{n}{2}, \dots, n\}_{ht}$ ; blue in Fig. 42,
- $\{(a_i, b_{\frac{n}{2}-4}), i = \frac{n}{2} + 5, \dots, n\}_{hh}$ ; dark blue in Fig. 42.

For  $p = \frac{n}{2} - k$ , with  $k \in \{5, 4, 3\}$ , page  $p$  of  $\mathcal{L}$  contains the following  $\frac{3n}{2} - 2k + 22$  edges:

- $\{(a_{p-1}, b_j), j = 2, \dots, \frac{n}{2} - p + 1\}_{ht}$ ; dark red in Fig. 43,
- $\{(a_p, b_j), j = \frac{n}{2} - p + 1, \dots, n - p + 2\}_{ht}$ ; red in Fig. 43,
- $\{(a_{p+1}, b_j), j = n - p + 2, \dots, n\}_{ht}$ ; light red in Fig. 43,
- $\{(a_i, b_{p+1}), i = \frac{n}{2}, \dots, \frac{n}{2} + (k-1)\}_{ht}$ ; pink in Fig. 43,
- $\{(a_i, b_{p+2}), i = \frac{n}{2} + (k-1), \dots, n - 8 + k\}_{ht}$ ; light pink in Fig. 43,
- $\{(a_{n-8+k}, b_j), j = \frac{n}{2} - 3 - k, \dots, \frac{n}{2}\}_{ht}$ ; blue in Fig. 43,
- $\{(a_i, b_{n+(2k-11)}), i = n - 8 + k, \dots, n\}_{ht}$ ; light blue in Fig. 43,
- $\{(a_i, b_{n+(2k-10)}), i = n - 8 + k, \dots, n\}_{hh}$ ; dark blue in Fig. 43,
- $\{(a_{n-8+k}, b_j), j = n + (2k-9), \dots, n\}_{hh}$ ; gray in Fig. 43.

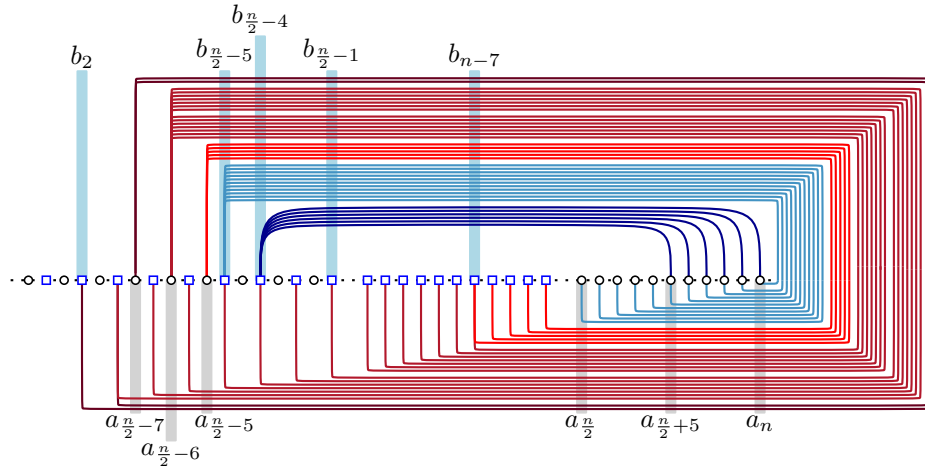


Figure 42: Page  $\frac{n}{2} - 6$  of  $\mathcal{L}$  when  $n$  is even.

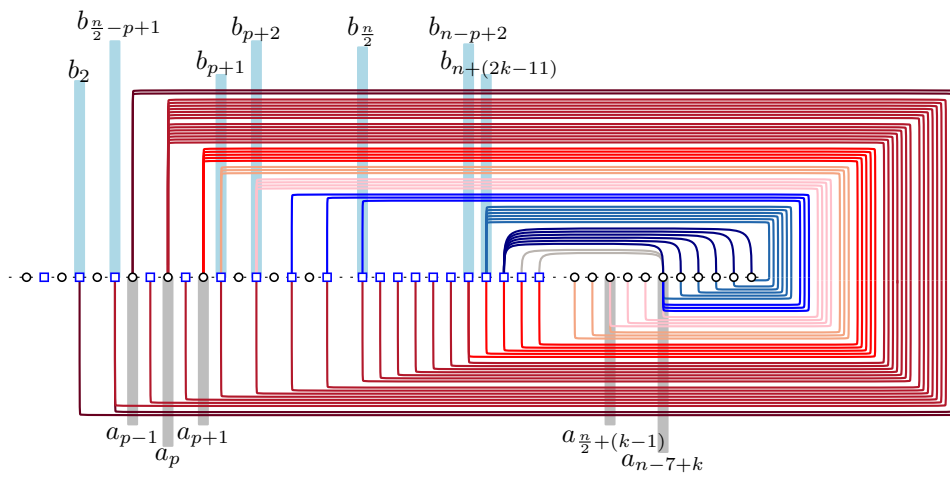


Figure 43: Page  $p = \frac{n}{2} - k$ , with  $k \in \{5, 4, 3\}$  of  $\mathcal{L}$  when  $n$  is even.

Page  $\frac{n}{2} - 2$  of  $\mathcal{L}$  contains the following  $\frac{3n}{2} + 19$  edges:

- $\{(a_{\frac{n}{2}-2}, b_j), j = 2, \dots, \frac{n}{2} + 4\}_{ht}$ ; dark red in Fig. 44,
- $\{(a_{\frac{n}{2}-1}, b_j), j = \frac{n}{2} + 4, \dots, n\}_{ht}$ ; red in Fig. 44,
- $\{(a_i, b_{\frac{n}{2}-1}), i = \frac{n}{2}, \frac{n}{2} + 1\}_{ht}$ ; light red in Fig. 44,
- $\{(a_i, b_{\frac{n}{2}}), i = \frac{n}{2} + 1, \dots, n - 7\}_{ht}$ ; pink in Fig. 44,
- $\{(a_i, b_{n-7}), i = \frac{n}{4} + 1, \dots, n\}_{ht}$ ; dark blue in Fig. 44,
- $\{(a_i, b_{n-6}), i = \frac{n}{4} + 1, \dots, n\}_{hh}$ ; light blue in Fig. 44,
- $\{(a_{\frac{n}{4}+1}, b_j), j = n - 5, \dots, n\}_{hh}$ ; gray in Fig. 44,
- $\{(a_{\frac{n}{2}-3}, b_j), j = 2, 3\}_{hh}$ ; blue in Fig. 44.

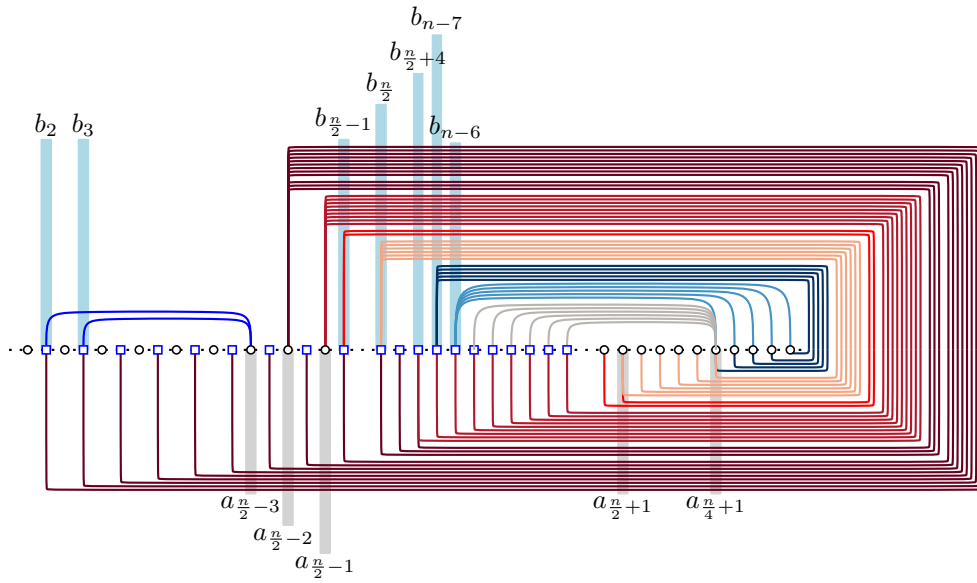


Figure 44: Page  $p = \frac{n}{2} - 2$  of  $\mathcal{L}$  when  $n$  is even.

So, in total  $\mathcal{L}$  has  $n^2$  edges. Since no two edges in the same rique deviate from the properties of cylindric layouts, it follows that the rique number of  $K_{n,n}$  is at most  $\frac{n}{2} - 2$  when  $n$  is even.  $\square$

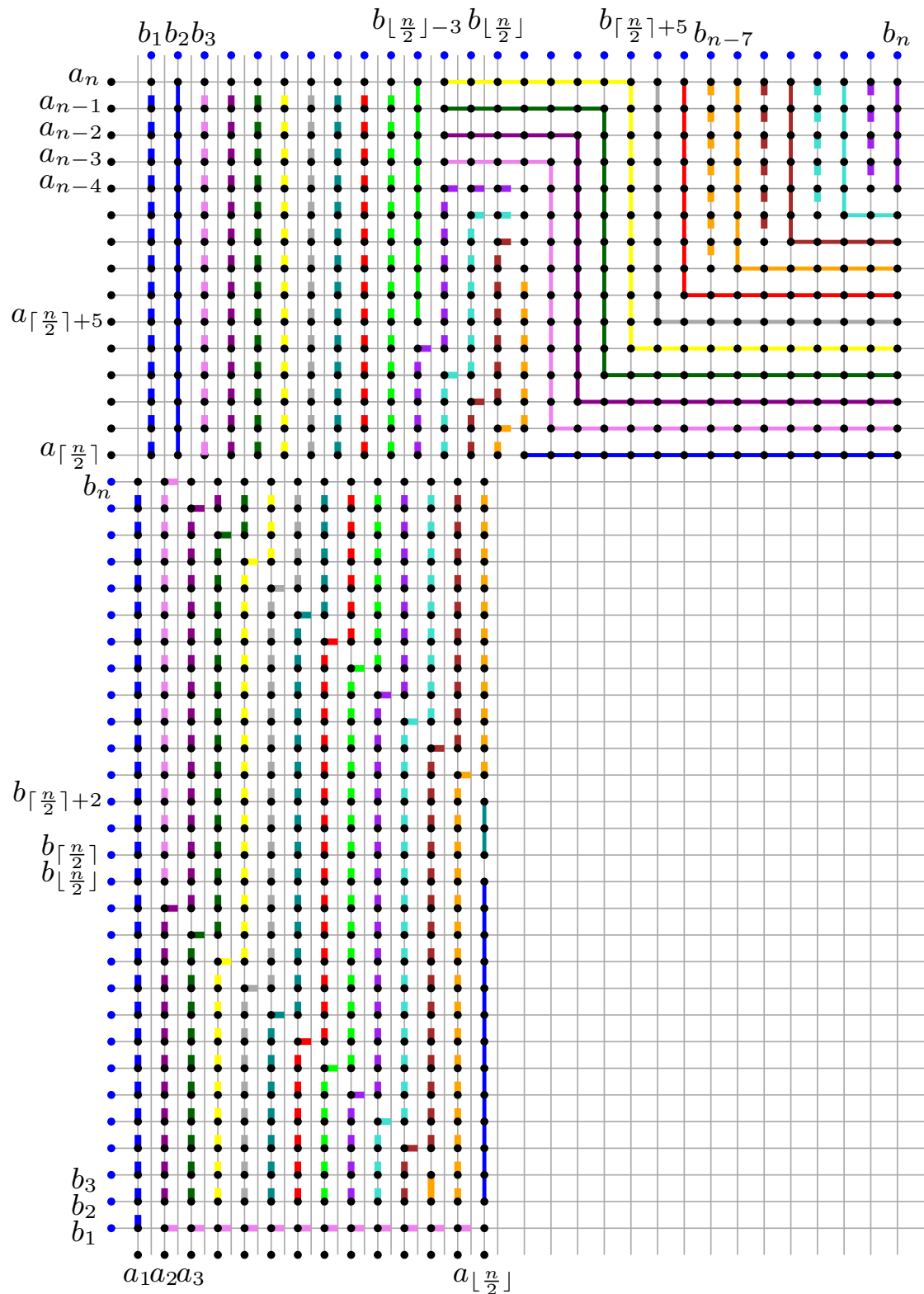


Figure 45: Illustration of the grid representation of a riqe layout of  $K_{n,n}$  when  $n$  is odd, in which paths of the same color correspond to the same rique. The points of the grid that are covered by a solid (dashed) path are head-head (head-tail, respectively). Here, the “special” pages are the first (blue), second (violet), third (dark-purple), fourth (dark-green), fifth (yellow), sixth (dark-gray), eighth (cyan),  $\frac{n-1}{2} - 5$  (green),  $\frac{n-1}{2} - 4$  (purple),  $\frac{n-1}{2} - 3$  (turquoise),  $\frac{n-1}{2} - 2$  (brown), and  $\frac{n-1}{2} - 1$  (orange) when  $n$  is odd.

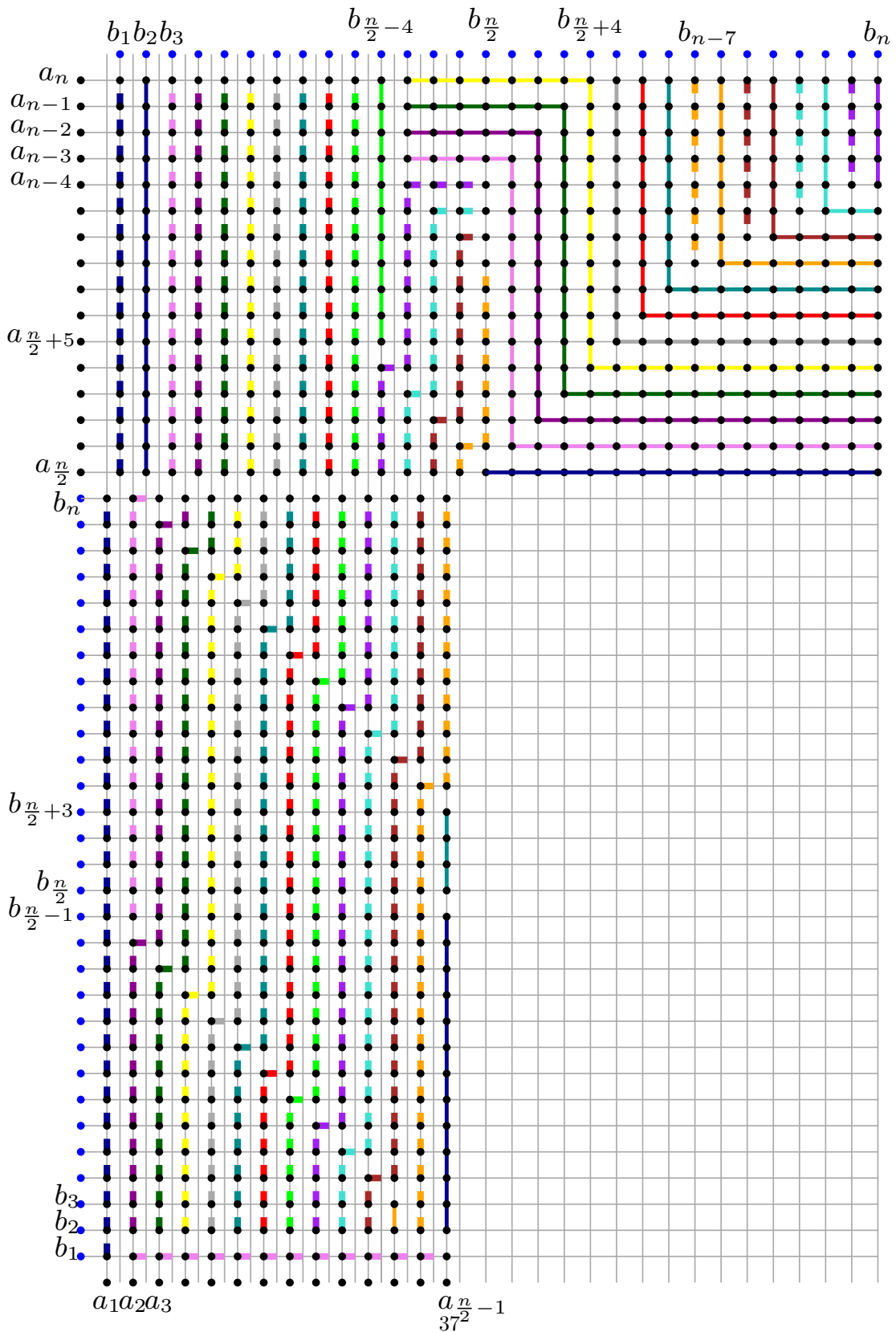


Figure 46: Illustration of the grid representation of a rique layout of  $K_{n,n}$  when  $n$  is even, in which paths of the same color correspond to the same rique. The points of the grid that are covered by a solid (dashed) path are head-head (head-tail, respectively). When  $n$  is even, the “special” pages are the first (blue), second (violet), third (dark-purple), fourth (dark-green), fifth (yellow), sixth (dark-gray), eighth (cyan),  $\frac{n}{2} - 6$  (green),  $\frac{n}{2} - 5$  (purple),  $\frac{n}{2} - 4$  (turquoise),  $\frac{n}{2} - 3$  (brown), and  $\frac{n}{2} - 2$  (orange).

## 5 SAT formulation

In this section, we present a SAT formulation for the problem of testing whether a given graph with  $n$  vertices and  $m$  edges admits a deque layout with  $p$  of dequeues; an implementation has already been incorporated in [5], whose source code is available at <https://github.com/linear-layouts/SAT>. However, before describing our formulation, we deem important to state that, in [4], Bekos et al. have already presented a corresponding SAT formulation, when the  $p$  pages are riques. However, their approach heavily relies on the fact that this specific type of linear layouts can be characterized by means of a forbidden pattern in the underlying order (similar to the corresponding ones for stack and queue layouts [7]). Given that dequeue layouts cannot be characterized by means of such forbidden patterns in the underlying order, we need a slightly different approach.

Similar to [4], our approach is an extension of the one in [7] for the stack layout problem, in which there exist three different types of variables, denoted by  $\sigma$ ,  $\phi$ , and  $\chi$ , with the following meanings: (i) for a pair of vertices  $u$  and  $v$ , variable  $\sigma(u, v)$  is **true**, if and only if  $u$  is to the left of  $v$  along the spine, (ii) for an edge  $e$  and a page  $i$ , variable  $\phi_i(e)$  is **true**, if and only if edge  $e$  is assigned to page  $i$  of the book, and (iii) for a pair of edges  $e$  and  $e'$ , variable  $\chi(e, e')$  is **true**, if and only if  $e$  and  $e'$  are assigned to the same page. Hence, there exist in total  $O(n^2 + m^2 + pm)$  variables, while a set of  $O(n^3)$  clauses ensures that the underlying order is indeed linear; for details see [7]. To overcome the issue that arises in the absence of forbidden pattern, we introduce  $4pm$  variables, such that variable  $\tau_i(e, x)$  with  $x \in \{hh, ht, th, tt\}$  is **true**, if and only if the type of edge  $e$  at page  $i$  is  $x$ . We ensure that each edge has at least one of the allowed types, by introducing the following clause for each edge  $e$ :

$$\bigvee_{i=1}^p (\tau_i(e, hh) \vee \tau_i(e, ht) \vee \tau_i(e, th) \vee \tau_i(e, tt))$$

With these variables, we can express different configurations that cannot occur in a deque layout as clauses in the SAT formula. These clauses are obtained by avoiding crossings between all edge types in the cylindric representation of the graph. E.g., to express the different configurations that cannot occur for a head-head edge  $e = (u, v)$  and a head-tail edge  $e' = (u', v')$ , we introduce the following clause for each page  $i$  of the layout<sup>3</sup>:

$$\begin{aligned} & \phi_i(e) \wedge \phi_i(e') \wedge \tau_i(e, hh) \wedge \tau_i(e', ht) \rightarrow \\ & \neg(\sigma(u, u') \wedge \sigma(u', v) \wedge \sigma(v, v')) \quad u \neq v \neq u' \\ & \wedge \neg(\sigma(v, u') \wedge \sigma(u', u) \wedge \sigma(u, v')) \quad u \neq v \neq u' \\ & \wedge \neg(\sigma(u, v') \wedge \sigma(v', v) \wedge \sigma(v, u')) \quad u \neq v \neq v' \\ & \wedge \neg(\sigma(v, v') \wedge \sigma(v', u) \wedge \sigma(u, u')) \quad u \neq v \neq v' \\ & \wedge \neg(\sigma(u, u') \wedge \sigma(u', v') \wedge \sigma(v', v)) \quad u \neq u' \\ & \wedge \neg(\sigma(u, v') \wedge \sigma(v', u') \wedge \sigma(u', v)) \quad u \neq v' \\ & \wedge \neg(\sigma(v, u') \wedge \sigma(u', v') \wedge \sigma(v', u)) \quad v \neq u' \\ & \wedge \neg(\sigma(v, v') \wedge \sigma(v', u') \wedge \sigma(u', u)) \quad v \neq v' \end{aligned}$$

We introduce a clause similar to the one above for each pair of types of edges, yielding in total  $O(pm^2)$  clauses. This completes the construction of the formula. Note that the formulation can

<sup>3</sup>Note that some parts of the clause appear only certain conditions apply on the endpoints of  $e$  and  $e'$ . These conditions are listed next to the corresponding parts, such that if a condition is not fulfilled, then the corresponding part has to be omitted.

be easily adjusted for rique layouts by introducing for each edge  $e$  and each page  $i$  the following clause forbidding tail-head and tail-tail edges:  $\neg\tau_i(e, th) \wedge \neg\tau_i(e, tt)$ .

Somehow unexpectedly, this simple adjustment was more efficient in practice than the one by Bekos et al. [4], which is based on implementing the forbidden pattern of rique layouts.

**Findings.** The implementation was extremely helpful, in general, for developing all upper bounds of this paper. It further shows that the upper bound of Theorem 5 is tight for all values of  $n \leq 30$  (see Remark 1). Another notable observation is that for  $K_{n,n}$  it is possible to obtain a better upper bound than the one of Observation 1 (or in other words that  $k$  dequeues are strictly more powerful than  $2k$  stacks): Our implementation shows that  $K_{3n,3n}$  with  $n \in \{2, 3, 4, 5\}$  needs  $n + 1$  stacks, while the solver provided solutions with  $n$  dequeues for the corresponding values of  $n$ . Note that this result would be implied (for any  $n$ ) by Theorem 6, if the bound [12] on the stack number of  $K_{n,n}$  was shown to be tight.

## 6 Open Problems

In this paper, we presented bounds on the deque- and rique-numbers of complete and complete bipartite graphs. We conclude with some open problems:

- (i) We conjecture that the bound of Theorem 5 is tight.
- (ii) As mentioned in the introduction, the deque-number of planar graphs is 2. We conjecture that also their rique-number is 2.
- (iii) Another natural direction to follow is to extend the study to other classes of graphs, as it is the case with the corresponding stack- and queue-numbers.
- (iv) Studying inclusion relationships is also of interest, e.g., the class of graphs admitting 1-deques is not a subclass of the class of graphs admitting 1-rique, 1-stack layouts, as a maximal planar graph with a Hamiltonian path plus an edge belongs to the former but not to the latter. What about the other direction?
- (v) Related to our research is also the problem of closing the gap between the lower bound of  $\lceil \frac{n}{2} \rceil$  and the upper bound of  $\lfloor \frac{2n}{3} \rfloor + 1$  [12] on the stack number of  $K_{n,n}$ .

## References

- [1] J. M. Alam, M. A. Bekos, M. Gronemann, M. Kaufmann, and S. Pupyrev. The mixed page number of graphs. *Theor. Comput. Sci.*, 931:131–141, 2022.
- [2] C. Auer. *Planar graphs and their duals on cylinder surfaces*. PhD thesis, Universität Passau, 2014.
- [3] C. Auer, C. Bachmaier, F. Brandenburg, W. Brunner, and A. Gleißner. Plane drawings of queue and deque graphs. In U. Brandes and S. Cornelsen, editors, *Graph Drawing*, volume 6502 of *LNCS*, pages 68–79. Springer, 2010.
- [4] M. A. Bekos, S. Felsner, P. Kindermann, S. G. Kobourov, J. Kratochvíl, and I. Rutter. The rique-number of graphs. In P. Angelini and R. von Hanxleden, editors, *Graph Drawing and Network Visualization*, volume 13764 of *LNCS*, pages 371–386. Springer, 2022.
- [5] M. A. Bekos, M. Haug, M. Kaufmann, and J. Männecke. An online framework to interact and efficiently compute linear layouts of graphs. *CoRR*, abs/2003.09642, 2020.
- [6] M. A. Bekos, M. Kaufmann, F. Klute, S. Pupyrev, C. N. Raftopoulou, and T. Ueckerdt. Four pages are indeed necessary for planar graphs. *J. Comput. Geom.*, 11(1):332–353, 2020.

- [7] M. A. Bekos, M. Kaufmann, and C. Zielke. The book embedding problem from a sat-solving perspective. In E. Di Giacomo and A. Lubiw, editors, *Graph Drawing and Network Visualization*, volume 9411 of *LNCS*, pages 125–138. Springer, 2015.
- [8] F. Bernhart and P. C. Kainen. The book thickness of a graph. *J. Comb. Theory, Ser. B*, 27(3):320–331, 1979.
- [9] V. Dujmovic, D. Eppstein, R. Hickingbotham, P. Morin, and D. R. Wood. Stack-number is not bounded by queue-number. *Comb.*, 42(2):151–164, 2022.
- [10] V. Dujmovic, G. Joret, P. Micek, P. Morin, T. Ueckerdt, and D. R. Wood. Planar graphs have bounded queue-number. *J. ACM*, 67(4):22:1–22:38, 2020.
- [11] V. Dujmović and D. R. Wood. On linear layouts of graphs. *Discrete Mathematics & Theoretical Computer Science*, 6(2):339–358, 2004.
- [12] H. Enomoto, T. Nakamigawa, and K. Ota. On the pagenumber of complete bipartite graphs. *J. Comb. Theory, Ser. B*, 71(1):111–120, 1997.
- [13] S. Felsner, L. Merker, T. Ueckerdt, and P. Valtr. Linear layouts of complete graphs. In H. C. Purchase and I. Rutter, editors, *Graph Drawing and Network Visualization*, volume 12868 of *LNCS*, pages 257–270. Springer, 2021.
- [14] J. L. Ganley and L. S. Heath. The pagenumber of  $k$ -trees is  $O(k)$ . *Discrete Applied Mathematics*, 109(3):215–221, 2001.
- [15] L. S. Heath, F. T. Leighton, and A. L. Rosenberg. Comparing queues and stacks as mechanisms for laying out graphs. *SIAM J. Discrete Math.*, 5(3):398–412, 1992.
- [16] L. S. Heath and A. L. Rosenberg. Laying out graphs using queues. *SIAM J. Comput.*, 21(5):927–958, 1992.
- [17] M. Hoffmann and B. Klemz. Triconnected planar graphs of maximum degree five are subhamiltonian. In M. A. Bender, O. Svensson, and G. Herman, editors, *ESA*, volume 144 of *LIPICs*, pages 58:1–58:14. Schloss Dagstuhl - Leibniz-Zentrum für Informatik, 2019.
- [18] P. Jungeblut, L. Merker, and T. Ueckerdt. A sublinear bound on the page number of upward planar graphs. In J. S. Naor and N. Buchbinder, editors, *ACM-SIAM SODA*, pages 963–978. SIAM, 2022.
- [19] D. J. Muder, M. L. Weaver, and D. B. West. Pagenumber of complete bipartite graphs. *J. Graph Theory*, 12(4):469–489, 1988.
- [20] T. Ollmann. On the book thicknesses of various graphs. In F. Hoffman, R. Levow, and R. Thomas, editors, *Southeastern Conference on Combinatorics, Graph Theory and Computing*, volume VIII of *Congressus Numerantium*, page 459, 1973.
- [21] A. Wigderson. The complexity of the Hamiltonian circuit problem for maximal planar graphs. Technical Report TR-298, EECS Department, Princeton University, 1982.
- [22] M. Yannakakis. Embedding planar graphs in four pages. *J. Comput. Syst. Sci.*, 38(1):36–67, 1989.
- [23] M. Yannakakis. Planar graphs that need four pages. *J. Comb. Theory, Ser. B*, 145:241–263, 2020.